Electromagnetic Science
vol. 1, no. 2, 0020111, June 2023
https://doi.org/10.23919/emsci.2022.0011

Review

Reconfigurable Intelligent Surfaces: Design, Implementation, and Practical Demonstration

Yijun Feng, Qi Hu, Kai Qu, Weixu Yang, Yilin Zheng, and Ke Chen

School of Electronic Science and Engineering, Nanjing University, Nanjing 210023, China

Corresponding authors: Yijun Feng, Email: yjfeng@nju.edu.cn; Ke Chen, Email: ke.chen@nju.edu.cn.
Received November 16, 2022; Accepted April 6, 2023; Published Online June 16, 2023.

Abstract — Metasurfaces, ultrathin two-dimensional version of metamaterials, have attracted tremendous attention due to their exotic capabilities to freely manipulate electromagnetic waves. By incorporating various tunable materials or elements into metasurface designs, reconfigurable metasurfaces and related metadevices with functionalities controlled by external stimuli can be realized, opening a new avenue to achieving dynamic manipulation of electromagnetic waves. Recently, based on the tunable metasurface concept, reconfigurable intelligent surfaces (RISs) have received significant attention and have been regarded as a promising emerging technology for future wireless communication due to their potential to enhance the capacity and coverage of wireless networks by smartly reconfiguring the wireless propagation environment. Here, in this article, we first focus on technical issues of RIS system implementation by reviewing the existing research contributions, paying special attention to designs in the microwave regime. Then, we showcase our recent attempts to practically demonstrate RIS systems in real-world applications, including deploying reflective RIS systems in indoor scenarios to enhance the wireless network coverage and utilizing intelligent omni-metasurfaces to improve both indoor and through-wall wireless communication quality. Finally, we give our own perspectives on possible future directions and existing challenges for RISs toward a truly commercial intelligent technology platform.

Keywords — Reconfigurable intelligent surface, Metasurface, Wireless communication.

Citation — Yijun Feng, Qi Hu, Kai Qu, *et al.*, "Reconfigurable Intelligent Surfaces: Design, Implementation, and Practical Demonstration," *Electromagnetic Science*, vol. 1, no. 2, article no. 0020111, 2023. doi: 10.23919/emsci.2022.0011.

I. Introduction

Controlling electromagnetic (EM) waves has been of interest for a long time and is widely used in current science and technology. For example, exploring flexible control of the propagation of wireless signals in a real three-dimensional (3D) space to form smart radio environments with programmable signal processing capabilities and channel modeling can lead to innovative communication systems in the future. EM wave propagation relies on the host medium in which the wave propagates and the specific boundaries formed by the interface between two regions. Considering these points, researchers have proposed the concept of a metamaterial, a kind of artificially engineered material composed of subwavelength structures, to provide a new platform for engineering materials exhibiting abnormal EM parameters such as zero permittivity, zero permeability, and a negative index. More recently, metasurfaces, the two-dimensional (2D) version of metamaterials, have emerged as a tool for wavefront engineering, with the advantages of low loss, low profile, low cost, etc. However, the static EM responses of passive metasurfaces still limit them when dynamic tuning of EM waves is required, for example, in beam scanning for target detection. Therefore, tunable, reconfigurable, and programmable metasurfaces have been proposed, which will soon evolve into intelligent metasurfaces integrated with sensors, feedback networks, and artificial intelligence (AI), responding smartly and automatically to environments to perform different tasks with less or even no human intervention. A schematic of the abovementioned concept progression is illustrated in Figure 1, focusing mainly on the evolution from metamaterials to metasurfaces and then to tunable metasurfaces and intelligent metasurfaces.

In the early stages, metamaterial research mainly focused on control and realization of effective medium parameters that cannot be found in naturally occurring materials. Such exotic EM parameters stem from the interactions between waves and subwavelength structures, typically termed the EM resonances of meta-atoms, leading to many unconventional physical phenomena and novel devices, such as negative refraction [1], invisibility cloaks [2], superlenses [3], and perfect absorption [4]. In a metamaterial, all the meta-atoms are usually formed with the same structure consisting of metallic/dielectric materials, which are then periodically arranged in 3D space. Although metama-

Electromagnetic Science

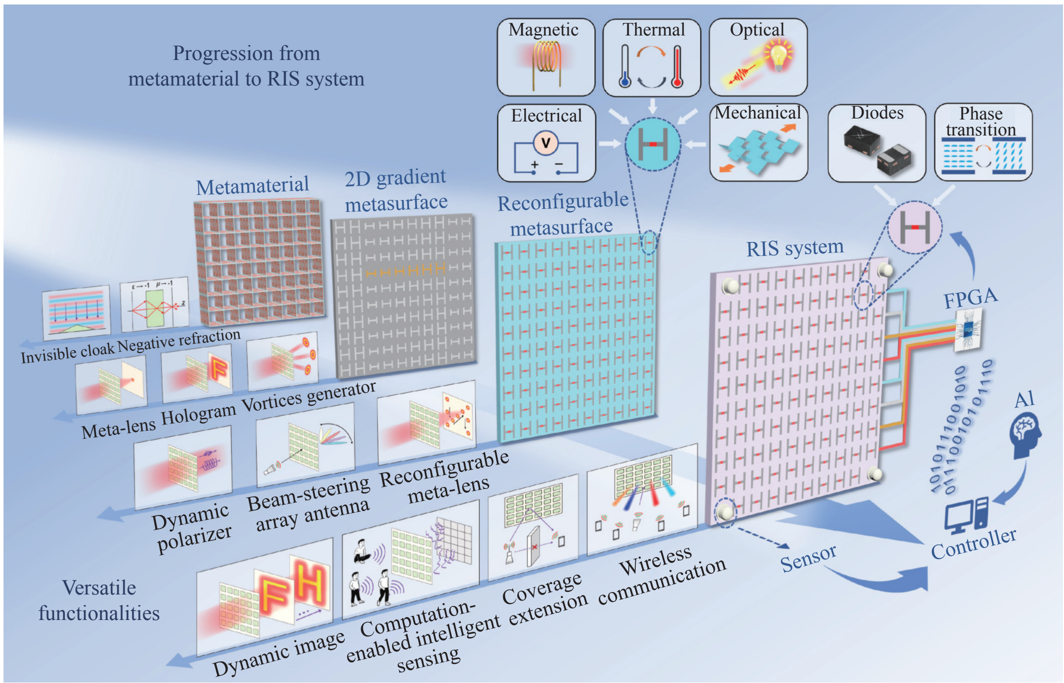

Figure 1 Development of metamaterials, metasurfaces, reconfigurable metasurfaces, and reconfigurable intelligent metasurfaces (RISs).

terials have introduced unprecedented capabilities in controlling the EM parameters and wave propagation, several challenges still exist, including bulky volumetric occupation, high cost, high insertion loss, and fabrication complexity, all of which undoubtedly limit their further developments and applications. Metasurfaces composed of planar subwavelength-sized structures with the designable EM responses have been proposed to overcome these issues [5]–[12]. Metasurfaces can be viewed as the 2D version of metamaterials that are typically arranged into a planar surface with specific spatially varying distributions of various meta-atoms, so they have the advantages of low profile, low cost, low loss, and easy fabrication. Moreover, unlike conventional metamaterials, whose wavefront tailoring is realized by phase accumulation of the wave propagating inside the media, metasurfaces introduce abrupt phase changes and thus field discontinuities across the interface between two media through engineering of the surface impedances of the constituent meta-atoms. Hence, by designing meta-atoms with a proper spatial variation, metasurfaces exhibit unconventional control of EM wave propagation and scattering and enable many inconceivable physical effects, such as anomalous refraction [12], anomalous reflection [13], and high-resolution holographic imaging [14]–[16]. Metasurfaces have also unlocked many intriguing functional devices and applications, such as skin cloaks [17], ultrathin metalenses [8], [18]–[21], special beam generation [22], [23], and metasurface antennas [24].

With the rapid development of metasurface research, passive metasurfaces have gradually shown limitations in practical applications because their wave-manipulation functionalities are static and fixed once designed or fabricated. Using proper multiplexing techniques such as polarization [25], [26], frequency [27]–[29] or direction [5], [30], [31] multiplexing, a single metasurface can integrate several wave functionalities; however, these functionalities are still static operations that cannot provide dynamic control. The capability to dynamically tune the wave functionalities will significantly improve the potential use of metasurfaces in real-world applications, which has gradually given rise to the concept of reconfigurable metasurfaces, including switchable, tunable, and programmable metasurfaces in recent years, to achieve dynamic control of EM waves nearly across the whole spectrum from the low microwave region to the terahertz and optical regions [8], [32]–[37]. Generally, reconfigurable metasurfaces should contain tunable materials or components that external stimuli can actively control. The main idea for realizing reconfigurable metasurfaces is the codesign of tunable components and resonant structures, where a change in external tunings can result in a change in the tunable components and, eventually, the overall EM behavior of the meta-atoms. Then, reconfigurable output functionalities are achieved by applying various control signals to form inhomogeneous metasurfaces with specific phase profiles. Driven by the promising perspective of tunable metasurfaces, many efforts have been devoted to exploring tunable components, including diodes [32], [38]–[42], graphene [43], [44], liquid crystals [45]–[48], and phase-change materials [49], that can be actively tuned by external stimuli of thermal effects [49], [50], electric voltage bias [32], [38]–[43], [51], mechanical actuation [52]–[54], etc. [55]–[58]. Reconfigurable metasurfaces of these kinds have been designed and implemented for different practical devices and applications, such as tunable lenses/imagers [8], [41], [42], [59], [60], dynamic beam shapers [61]–[63], reconfigurable antennas [64]–[67], and on-demand polarizers [68]–[72]. In addition, reflectarray and transmitarray antennas can perform similar dynamic wave functionalities due to the tunable components (e.g., diodes) in the constituent elements [73]–[79]. The reconfigurable surface in an antenna system is designed to dynamically reshape the incident wave from a particular feed antenna placed near the surface. Overall, reconfigurable surfaces pose many challenges in the design and fabrication process because appropriate strategies to make structures with a tunable performance in a given frequency domain should be found, while an additional bias network or control system would further increase these difficulties, especially for the cases of individually addressable elements, high-frequency operation, and surfaces with large-scale elements.

More recently, reconfigurable metasurfaces have further evolved into reconfigurable intelligent metasurfaces (RISs) and RIS-based systems, providing a smart paradigm for EM wave manipulation [52], [59], [60], [80]–[106]. A typical RIS comprises a reconfigurable metasurface, a software and hardware control system, and sensing or feedback components, which are often integrated with algorithms to enable self-adaptivity via their reprogrammable wave functionalities, with less or even no human intervention. From the viewpoint of output wave functionalities, an RIS is similar to a reconfigurable metasurface, both of which can exhibit dynamic reflection/transmission EM responses to form tunable inhomogeneous profiles at the metasurface apertures. However, RISs make strides toward intelligent control of EM waves: the sensing and feedback components act as the "eyes" to see the environment or meet the requirements, while onsite or cloud algorithms act as the "brains" to determine their output EM behavior. Hence, RISs have strong self-decision capabilities in which they can intelligently perform a series of successive software/algorithm-defined tasks, such as smart beam shaping [85], adaptive retroreflection [52], and gesture recognition [59], [89]. Although RIS research has been widely performed across nearly the whole spectrum, thus far, most of the reported RISs are aimed at engineering microwaves for the following reasons. First, the necessary physical basis for constructing such RISs is comparatively mature. Commercial diodes can provide very fast switching or continuously tunable speeds and are well compatible with the output voltages from widely used controllers, for example, field-programmable gate arrays (FPGAs), while the standard printed circuit board (PCB) process provides mature technology for large-scale sample fabrication. The FPGA controller supports parallel communication and output voltages, enabling the phase profiles of massive meta-atoms to synchronously switch from one to another. Second, RISs have emerged as a new technology for the next generation of wireless communication and may solve problems in real-world applications. In the current wireless communication scheme, microwave propagation cannot be controlled and customized after the waves are emitted from the sources and before the terminals receive them. Recent studies show that RISs can be used to build a dynamically controllable smart wireless environment by simply placing them on large scatter (e.g., buildings) surfaces. RISs provide real-time software-defined EM responses that can fully use the propagation effect of EM waves and thus maximize the performance of entire communication networks in terms of extending the signal coverage and improving the quality of received signals [87], [88], [90]–[111]. They also enable metasurface-assisted wireless communication by modulating the transmitted information directly based on the EM performance of the metasurface [112]–[116]. As a long-term prospect, the RIS-based platform is envisioned to perform joint tasks as much as possible, such as communication, sensing, localization, computing, signal processing, and automatic learning, with low cost, high throughput, and high reliability. Overall, RISs gradually evolved from metamaterials, metasurfaces and reconfigurable metasurfaces, so they have the advantages of the previous artificially engineered materials. Nevertheless, the more advanced the capabilities or more versatile the wave functionalities demanded are, the more challenges RISs need to overcome, together with the pressing demands from the application side, because one should consider the codesign of several parts far beyond material engineering.

This article reviews recent research advances in this field, focusing mainly on designs in the microwave regime with an emphasis on our own work. After a comprehensive comparison of reconfigurable metasurface implementations with electrical, thermal, mechanical, and other tuning mechanisms, we highlight the experimental implementations of RIS systems by exhibiting their practical uses in dynamic wave control, local wireless signal enhancement, etc. Finally, we conclude this review, followed by our viewpoints on the challenges in this emerging interdisciplinary research area and perspectives on this field's future developments.

II. Implementations of Reconfigurable Metasurfaces

There are many approaches to realize reconfigurable metasurfaces, which depend on the different working mechanisms of tunable meta-atoms. By including stimuli-responsive materials in their designs, meta-atoms may undergo relatively large and rapid changes in their physical properties in response to external ambient stimuli [80], [117]–[123]. In this case, when enacting external control based on the ambient conditions, such as biasing with an external current or voltage, applying an electric/magnetic field, heating or cooling with temperature changes, exerting mechanical pressure, or providing light illumination, the material properties and the interaction between the meta-atom and the EM wave will be tuned accordingly and therefore induce a change in the metasurface functionality.

1. Different tuning mechanisms

In Figure 2, we briefly summarize the different tuning mechanisms that have been applied in current implementations of reconfigurable metasurfaces as well as the corresponding external stimuli used to actively control the dynamic modulation of metasurfaces.

Both global and local tuning can be achieved through these mechanisms to realize reconfigurable EM properties of the whole metasurface or each individual meta-atom, respectively. In the local tuning scenario, more reconfigurable functions, such as EM beam steering, dynamic focusing, imaging and holography, can be achieved, but external stimuli should be applied locally to each meta-atom. Realizing local tuning through thermal, optical, and magnetic means for reconfigurable meta-atoms is quite difficult and complicated due to the additional large objects compared to the unit cell size that need to be involved in the unit-cell design even in the microwave range. However, electrical control utilizing PIN diodes, varactors or micro-electromechanical system (MEMS) switches, which have comparably small sizes and simple biasing circuits, can be easily implemented in reconfigurable metasurfaces even with very many individually tunable unit cells and large physical sizes [83].

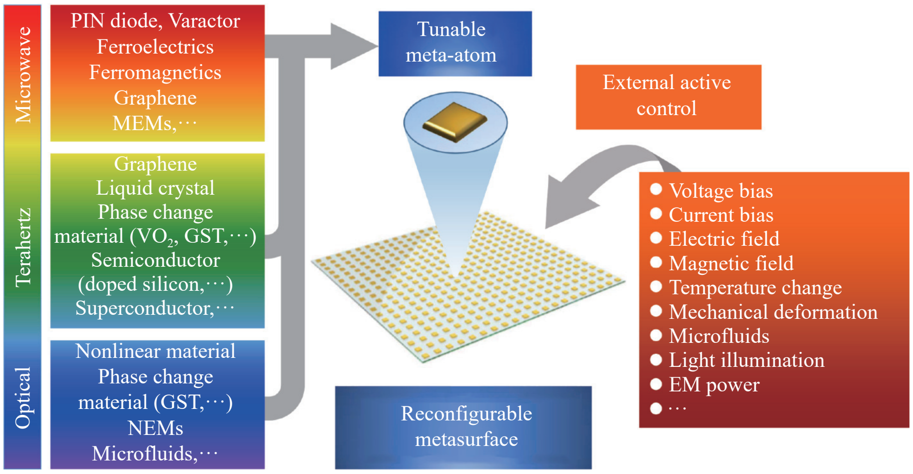

Figure 2 Different mechanisms to implement reconfigurable metasurfaces.

Table 1 ([39], [46], [48], [52], [53], [56], [124]–[158]) summarizes most of the stimuli-responsive mechanisms that have been used to realize tunable and reconfigurable metasurfaces in different operating regimes from megahertz to optical frequencies through various external stimuli. Reconfigurable functionalities, such as tunable absorbers or polarizers, dynamic beam forming or steering, dynamic lenses or holograms, tunable scattering or retroreflection, information modulators and wireless communication, can be achieved utilizing these approaches via electrical, thermal, optical, magnetic or mechanical control. Among various external stimuli, electrical control is largely used, as there are many electrically sensitive materials, including nematic liquid crystals (LCs), doped indium tin oxide (ITO) and aluminum-doped zinc oxide [48], [124]–[127]. Semiconductors, 2D materials (e.g., graphene), and transparent conductive oxides (TCOs), such as electric circuit elements, e.g., PIN diodes and varactors, can also be loaded into meta-atoms whose EM characteristics (e.g., capacitance) can be dramatically tuned by applying various voltages [39], [128]–[132]. Phase-change materials (PCMs), such as germanium-antimony-telluride ($Ge_2Sb_2Te_5$, also called GST) and vanadium dioxide (VO_2), which exhibit reversible phase transitions with significant changes in their refractive index, can be embedded in meta-atoms to realize tunable functions upon local temperature changes induced by electrical heating [133]–[136]. For example, an electrically driven reconfigurable metasurface based on GST could achieve an eleven-fold change in the reflectance (absolute reflectance contrast reaching 80%) and quasi-continuous spectral tuning over 250 nm [136].

Photoconductive semiconductor materials, such as Si and GaAs, can be employed for implementing reconfigurable metasurfaces by tuning their conductivity through carrier photoexcitation under optical injection [137], [138]. The first reported optically controlled metasurface was a patterned copper split-ring resonator (SRR) array on a GaAs substrate, which demonstrated that under ultrafast light pumping at 800 nm, the photoexcitation-induced conductivity in GaAs can provide strong modulation of the transmission amplitude of a terahertz wave [137]. In a diffractive array of GaAs semiconductor resonators that support both dipolar and quadrupolar Mie resonances, through optical injection of free carriers to spectrally shift the multipoles and rebalance the multipole strengths, radiation into a diffraction order is enabled on an ultrafast timescale [138]. Graphene-based thin films can also be employed to realize absorption modulators for operation in the THz regime with ultrafast optical control. Modulation of absorption on the order of 40% within a few picoseconds has been achieved by applying an optical pump signal, which modifies the conductivity of the graphene sheet [139]. Ultrafast plasmon modulation in the near-infrared (NIR) to mid-infrared (MIR) range was successfully

Table 1 Summary of different approaches to realize tunable and reconfigurable metasurfaces

External stimuli	Tuning mechanism	Operation regimes	Materials	Function	Frequency	Ref.
Electrical	Carrier doping	GHz to Visible	Semiconductors	Modulator	0.81/0.89 THz	[124]
			Graphene	Dynamic scattering	12.9–13.9 GHz	[125]
			TCO	Beam steering/Lens	1.5–3 μm	[126]
	Phase transition	GHz to Visible	Liquid crystals	Beam steering	32.5 GHz	[127]
				Beam steering	0.67 THz	[48]
			VO_2	Modulator	1.2–2 μm	[133]
				Dynamic imaging	0.42–0.48 THz	[134]
			GST	Modulator	0.5–0.8 μm	[135]
				Modulator/Beam manipulation	1.4–1.7 μm	[136]
	Capacitance	MHz to GHz	PIN diodes	Tunable scattering	2.1–2.9 GHz	[39]
				Dynamic beam manipulation	6/9.8 GHz	[128]
				Dynamic beam manipulation	9.5–11.5 GHz	[129]
			Varactors	Dynamic metalens	6.7–7.1 GHz	[130]
				Beam steering	3.15 GHz	[131]
				Tunable absorber	4–5.3 GHz	[132]
Optical	Carrier doping	THz to Visible	Semiconductors	Modulator	0.56 THz	[137]
				Dynamic beam manipulation	1–1.1 μm	[138]
			Graphene	Tunable absorber	2.2 and 6.5 THz	[139]
			TCO	Modulator	1.4–2.2/3.5–5 μm	[140]
				Modulator/Polarizer	0.5–0.9 μm	[141]
	Phase transition	THz to Visible	VO_2	Modulator	0.41 and 0.8 THz	[142]
			GST	Dynamic lens/Hologram/Modulator	3.75 μm	[143]
				Modulator	0.72–1.13 THz	[144]
	Light-microwave transmitter	GHz	Photodiode & Varactors	Dynamic cloak/Vortex beam	5.62–6.62 GHz	[56]
				Wireless communication	4–6.3 GHz	[145]
Thermal	Phase transition	THz to Visible	GST	Dynamic beam/Lens	3.1 μm	[146]
			Liquid crystals	Dynamic beam steering	0.75–0.8 μm	[46]
			VO_2	Tunable absorber	5–20 μm	[147]
				Modulator	1.35–1.65 THz	[148]
			Superconductor	Modulator	0.2–0.5 THz	[149]
			Semiconductor	Modulator	1.4–1.5 μm	[150]
Magnetic	Magnetostatic field	GHz to Visible	Ferrite (YIG)	Nonreciprocal shift	4.76 GHz	[151]
				Tunable absorber	8–12 GHz	[152]
			InAs	Tunable absorber	0.1–5 THz	[153]
			PDMS/Fe	Tunable reflector	0.7–1 μm	[154]
Mechanical	Mechanics	GHz to Visible	Micromotor	Retroreflector	3.7–4.6 GHz	[52]
			MEMS/NEMS	Modulator	1.2 and 1.6 μm	[155]
			Structural deformation	Tunable lens	7.8–18 GHz	[53]
				Tunable lens	0.6 μm	[156]
			Microfluids	Retroreflector	15 GHz	[157]
				Tunable colors	0.5–0.6 μm	[158]

demonstrated by intraband pumping of a metasurface composed of ITO nanorods, providing a useful method of optical tuning by tailoring the ITO metasurface geometry [140], [141]. By combining a varactor with a photodiode, a digital metasurface based on electronic varactors integrated with an optical interrogation network can convert visible light illumination patterns to voltages and apply a bias to the metasurface elements, which could provide an interesting approach to generate specific phase distributions for realization of various wavefront tailoring devices and direct wireless communication [56], [145].

Thermal control is another candidate for the ambient stimulus for reconfigurable metasurfaces, where PCMs with temperature-dependent permittivity are often employed in tunable meta-atom design. For example, VO_2, as a commonly used PCM, could behave as an insulator at room temperature and change to a metallic state at higher temperatures due to the enhancement of the free carrier concentration. It has been utilized to design a tunable meta-atom to shift its resonance frequency and modulate the transmission amplitude via direct substrate heating [147], [148]. Chalcogenide PCMs such as GST have also been employed in tunable metasurface design, where the GST layer can be partly switched from the amorphous to crystalline state to generate intermediate refractive indices enabling beam switching and bifocal lensing [146]. In addition, superconductor materials are also employed to design tunable metasurfaces, as their conductivity strongly depends on temperature, which may induce the transition from a superconducting state to a normal state. By designing an SRR array with a high-temperature superconducting film [149] or a niobium nitride film [159], efficient metamaterial resonance switching or transmission modulation can be realized by varying the ambient temperature.

Other tuning approaches, including magnetic and mechanical control, are summarized in Table 1. Magnetically responsive structures have been explored through ferrite-based metasurfaces to provide a magnetically controllable nonreciprocal Goos-Hänchen shift enabled by magnetic plasmonic gradient metasurfaces consisting of an array of ferrite rods [151] or magnetically tunable perfect absorption based on ferromagnetic resonance with a tunable working frequency controlled by the applied magnetic field [152]. Magnetic field-driven polymer microplate arrays have also been proposed to modulate the optical properties by magnetically controlling the tilt angle of the microplates to reversibly switch their surface reflectivity from a higher to lower state [154]. Dynamically reconfigurable metasurfaces can also be realized by mechanically changing the geometries of the constituent meta-atoms or altering the distances between adjacent meta-atoms. For example, MEMSs or nanoelectromechanical systems (NEMSs) are employed to realize tunable metasurfaces either in microwave and terahertz bands or in optical frequency ranges, respectively [155], [160]. A reconfigurable omnidirectional adaptive retroreflector has been realized by dynamically and continuously controlling the reflection phase of constituent meta-atoms through alteration of their orientation states, which can be individually mechanically addressed with a tiny micromotor connected to each meta-atom [52]. Metasurfaces fabricated on flexible or stretchable substrates can offer a direct way to enact reconfigurability upon mechanical deformation of the structures [53], [156]. In this scenario, both origami- and kirigami-based structures could be useful solutions to create deployable continuous-state tunable metasurfaces in which a folding pattern enables a change of the overall structure shape or periodicity of the meta-atoms, thereby realizing on-demand reconfigurability. For example, a kirigami-based reconfigurable gradient metasurface has been proposed and successfully applied in designing a metalens with a tunable focal length or chromatic aberration-free focusing [53]. An origami metawall has been designed and demonstrated with reconfigurable functions of an absorber, a mirror, or a negative reflector depending on mechanical stretching or compression of the structure [161].

Most of the above discussed tuning mechanisms can be applied to different frequency bands from the microwave to optical range. In particular, achieving reconfigurable metasurfaces for applications from gigahertz to a few terahertz is relatively easy, and the control methods to address each meta-atom to realize spatial variation of the EM properties of the metasurface are more practical and can mostly be implemented with external electrical stimuli. In the next sections, we will focus on the designs and implementations of microwave reconfigurable metasurfaces and their practical applications.

2. Microwave reconfigurable metasurfaces

In the microwave frequency regime, PIN diodes, varactors, and other voltage-driven circuit elements have been widely used to design tunable meta-atoms to achieve reconfigurable EM functionalities, as they have compact sizes so can be easily embedded in the passive metallic meta-atom structure. Although PCMs such as liquid crystals or graphene sheets have also been employed in microwave tunable metasurfaces, they are comparably complicated in the realization of external control, especially for large-scale metasurfaces with individual meta-atom addressing [125], [162].

Figure 3 shows a design example of a reconfigurable reflective metasurface for achieving 1-bit phase control for dual-polarization incident EM waves [40]. The meta-atom shown in Figure 3(a) has a metallic resonant structure with central and rotational symmetry, which can respond to dual polarization and can maximally suppress the cross-polarization level of the reflected waves. Four PIN diodes are symmetrically loaded into the meta-atom to realize a 1-bit element with the features of high efficiency, programmability, and independent dual-polarization control, where both dual-polarized reflection phases can be dynamically switched between 0° and 180° under DC current biasing. The diodes connecting the central patch to the four side patches (top metallic layer) are independently biased through metallic vias from the ground plane (middle metallic layer) and bottom layer. The ground plane acts as one electrode, and the biasing network (bottom metallic layer) under the ground plane acts as the other electrode, thus enabling each element to work independently in both polarization channels. Placing the ground plane between the resonant layer and the biasing layer could remarkably weaken the deterioration effect of the dense metallic bias lines on the overall reflection response of the metasurface element, which is often used in tunable reflective metasurface design. The simulated reflection phases and amplitudes are shown in Figure

3(b), which illustrate that the phase difference is approximately 180° between the two working states, and the reflection amplitudes are all over 0.96 within the operation bandwidth with a center frequency of 7.45 GHz. More importantly, the reflection response of the meta-atom only depends on the PIN diodes welded in the parallel direction under specific polarized waves and is not affected by the working states of PIN diodes in the orthogonal direction, enabling independent phase control of both polarization channels.

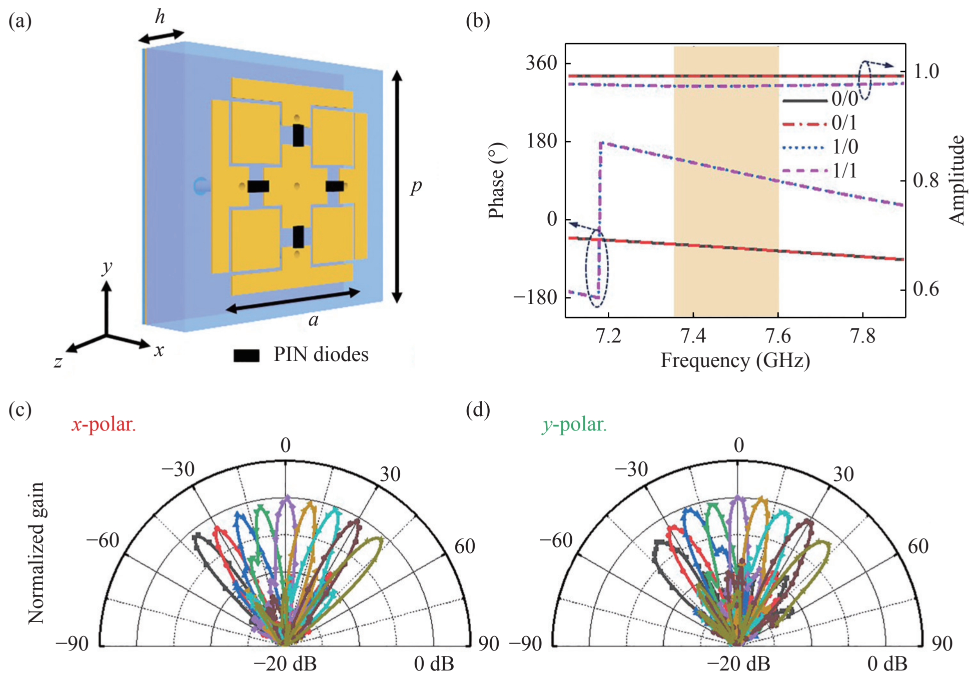

Figure 3 One-bit reconfigurable metasurface for dual polarization [40]. (a) Schematic of the dual-polarized coding metasurface elements; (b) Simulated reflection phases and amplitudes. The numbers before and after the slashes (/) represent the coding states along the z- and y-directions. Measured radiation patterns for beam scanning from −40° to 40° with a 10° step at 7.45 GHz in the (c) z-polarization channel and (d) y-polarization channel.

As an application of the 1-bit programmable metasurface, a reconfigurable reflectarray (RRA) with independent dual-polarized beam steering has been demonstrated. The RRA is entirely driven by the external digital signals from the FPGA-based hardware system. By addressing each meta-atom with an independent DC voltage to achieve different spatial phase distributions, wide-angle beam scanning is obtained in dual-polarized channels, with low cross-polarization levels and acceptable side lobe levels, as shown in Figures 3(c) and (d). The measured results show that wide-angle beam scanning up to ± 40° can be obtained at approximately 7.45 GHz, with peak gains of 21.13 dBi and 20.89 dBi in the dual channels, corresponding to aperture efficiencies of 16.35% and 15.47%, respectively. Such a dual-polarized RRA may provide a new method for multi-beam antenna design, which will be conducive to the realization of the large-scale multiple-input multiple-output (MIMO) antennas for 5G technology [163]. In addition, the dual-polarization working mode will highly enhance the storage densities and information capacities of the systems, offering potential capabilities of fast information communication and detection.

Unlike PIN diodes that can only be switched between two states, varactor diodes can be adjusted to achieve a continuously varying capacitance upon changing the reverse bias voltage, which have been widely investigated for realizing continuously tunable metasurfaces, such as the microwave absorbers with a tunable working bandwidth or tunable absorption [132], [164] or reconfigurable metalenses with a tunable focal length or a dynamic focal point [130]. The typical capacitance range for commercially available varactor diodes can be a few pico-Farad, e.g., 0.5–3.5 pF in the GHz frequency band under a bias voltage ranging from 0 V to 20 V. By embedding varactors in meta-atoms, continuous phase manipulation can be obtained via voltage control that may cover the full range of 360°, which can be easily utilized to achieve 1- and 2-bit or even multibit phase states for more complicated EM wavefront or beam forming control.

Although utilizing PIN diodes or varactor diodes is the most widely used approach to realize microwave reconfigurable metasurfaces with fast switching between different phase states, the insertion loss caused by electronic devices can lead to deterioration of the operation efficiency. Another issue is that the operation of these diode-embedded metasurfaces always requires a power supply, which may increase energy consumption, especially for large-scale metasurfaces with many elements. To overcome these challenges, an alternative strategy of controlling the tunable element via mechanical devices, such as micromotors [52],

[165], piezoelectric actuators [166], and spring devices [167], is gradually emerging for microwave reconfigurable metasurfaces. A higher phase resolution can be effectively achieved by continuously performing rotational operations [52], [168], [169] on the tunable element or changing the height/thickness [166], [168], [170] in the structure (changing its resonance properties or optical path difference) via suitable mechanical devices.

As a simple example, we show a typical design of a reflective metasurface mechanically controlled by tuning the thickness of an air layer. As shown in Figure 4(a), the unit cell is designed in the S-band with a center frequency of 2.55 GHz. For each unit cell, 4 × 4 square metallic patches evenly distributed on a dielectric substrate serve as the resonant structure. A movable metallic ground controlled by a stepping motor is set behind the dielectric substrate. Hence, the air thickness *h*, i.e., the distance between the movable metallic ground and the dielectric substrate, can be continuously modulated by the stepping motor. The entire metasurface shares a fixed dielectric substrate printed with periodic metallic patches, as illustrated in the fabricated prototype shown in Figure 4(b). Notably, this mechanically controlled RIS possesses both high efficiency and continuous phase modulation with a full range of over 360°, as shown in Figure 4(c). For practical implementation, the stepping motor of each unit cell is operated by an independent DC voltage and controlled by an FPGA (shown in Figure 4(d)). The greatest advantage of this mechanically controlled reconfigurable metasurface is that it only needs to be powered when switching between different tuning states for beam shaping requirements, which is potentially suitable for some application scenarios that require high energy conservation but not high reconfiguration frequency, such as indoor signal enhancement and wireless power transfer.

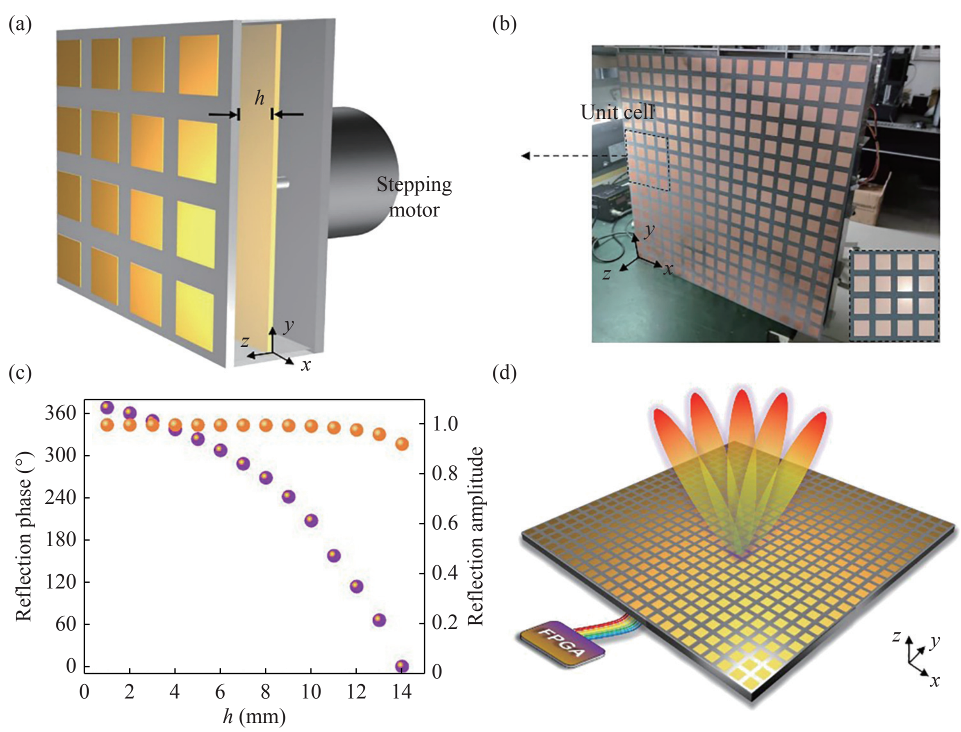

Figure 4 Mechanically controlled reconfigurable metasurface with a tunable air thickness. (a) Proposed structure of the unit cell; (b) Photograph of the fabricated prototype; (c) Simulated amplitude and phase responses versus the air thickness; (d) Schematic of the operation mode of the mechanically controlled metasurface.

III. Practical RIS Systems and Demonstrations in Wireless Communication

An RIS is a 2D metasurface structure that is reconfigurable in terms of its functionality when interacting with propagating EM waves. Practical RIS systems are mainly composed of reconfigurable metasurfaces integrated with tunable or switchable meta-atoms to realize passive EM wave manipulation with controllable wavefront, intensity, polarization and beam direction. Various dynamic EM wave responses can be enacted by reconfigurable metasurfaces through an intelligent control system with a microprogrammed control unit (MCU) or FPGA to directly program the states (reflection or transmission phase, magnitude, polarization) of each meta-atom with different spatial coding sequences in a real-time control manner. By judiciously designing and implementing the RIS system, the incident EM wave signals can be manipulated through either a reflection [83] or transmission [130] channel, or even both channels [171], with high design freedom in the wave propagation direction, polarization, and intensity. For example, an RIS can focus the incident EM power to predesigned areas to change the wave intensity distribution and increase certain local signal coverage. Owing to their capability for proactive EM wave manipulation, RIS systems have been recognized as a key technology to modify the wireless communication environment and have become a hotspot of research in wireless communications to achieve smart and reconfigurable wireless channel/radio propagation environments for next-generation wireless communication systems [87], [88], [90], [92], [172]. By deploying RIS systems and smartly coordinating their wave interaction properties, the wireless channels between transmitters and receivers can be flexibly reconfigured to circumvent obstacles and fulfil an enhanced received signal at the terminal devices, which may provide a fundamental way to tackle wireless channel fading and interference issues and potentially improve the wireless communication capacity and reliability. RISs possess many advantages, such as easy implementation and deployment, spectral efficiency enhancement through the construction of a software-defined wireless environment, greater energy efficiency and environmental friendliness than conventional relaying systems, and compatibility with the standards and hardware of existing wireless networks.

1. Practical considerations and requirements of RIS systems

For applications in wireless communication scenarios, the main practical consideration is the hardware implementation of the RIS system, including both the reconfigurable metasurface and its electronic controller. Many issues influence the performance of RISs, such as the maximum number of meta-atoms in the metasurface with all integrated bias circuitry for individual addressing, the number of quantization levels of the RIS phase or magnitude responses, and the percentage of the scattering environment that can be coated by an RIS. The deployment of an RIS system is often limited by the tradeoffs caused by the hardware constraints based on analyzing their effect on the channel modification [173], the complexity and power consumption of the control system, and performance metrics such as the outage probability [174] and ergodic capacity [175].

Table 2 ([40], [59], [82], [85], [115], [116], [131], [171], [175]–[185]) summarizes the recent experimental demonstrations and prototypes of RIS systems. Various tunable functions have been demonstrated with RIS systems, such as the dynamic EM beam steering and focusing used in RIS-assisted wireless communication to adaptively modify the propagation channel and improve the performance and the signal modulation through the phase, magnitude or polarization of the output EM wave that may enable a direct-signal-modulation transmitter for a new architecture of wireless communication. Most reconfigurable metasurfaces utilize PIN diodes as tunable or switching elements in meta-atoms to achieve one- or two-bit phase modulation for easy and robust control with simple digital control circuitry. Although multibit phase quantization may provide more freedom in EM wavefront manipulation, recent theoretical studies indicate that a one-bit coding RIS system may yield satisfactory performance in most practical scenarios in terms of the resulting channel cross-talk and reduction of the information capacity in wireless communication [102].

The working frequency bandwidth of an RIS for passive beam forming of wireless signals via reflection or refraction is dominated by the reconfiguration mechanism of the meta-atoms interacting with the EM waves. In most cases, tunable EM resonance is employed to enact phase shifts or magnitude variations to reconfigure the wireless signals output from the RIS through external electrical biasing. Such EM resonance may possess a strong dispersive nature and limit the signal frequency to a single working band. However, by judiciously designing meta-atoms with multimode resonance through interleaved or multilayered structures, broadband or multiband RISs can be achieved. For example, a 1-bit high-efficiency programmable metasurface with a bilayer structure has been reported to achieve completely independent functions with real-time reconfigurability in both the C-band and X-band [128].

The switching speed between different phase or magnitude states in each element of the reconfigurable metasurface is also an important characteristic that is dominated by the response time of the tunable element used in the meta-atom. PIN diodes and varactors are the most commonly used devices in the microwave region for reconfigurable meta-atom phase or amplitude, which have much faster dynamic responses than other methods, such as utilization of mechanical actuators, liquid crystals, or PCMs [186]. A switching time for beam forming within several tens of nanoseconds can be obtained by employing microwave PIN diodes, which is sufficient for RIS-assisted wireless networks [92]. For the application of an RIS-based direct-signal-modulation transmitter, increasing the switching speed through innovative designs is required to achieve a much better data rate.

In addition to the EM properties and architecture design of RIS systems, both the software of efficient algorithms for channel estimation and signal processing and the hardware for controlling signals are key design aspects that need to be considered and realized with low power consumption and low complexity. To enable the flexible deployment of RISs, the inherent limitations of wired lines and power lines for controlling them cannot be underestimated. In most demonstrated RIS systems, computer-controlled FPGAs or microcontrollers are involved to provide highly reliable and easily implementable signal and data processing. However, many issues, including signal integrity, power consumption, and remote control, still need to be properly resolved.

2. One-bit reflective RIS systems

By deploying RIS systems in the environment, e.g., coated on the walls of buildings or rooms, they can bring additional phase shifts to the reflected signals, and by jointly optimizing the phase shifts of all scattering elements, namely, passive beamforming, the signal reflections can be coherently focused at the intended receiver and nulled in other directions. Thus, a smart radio environment can be estab-

Electromagnetic Science

Table 2 Summary of experimental demonstrations and prototypes of RIS systems

Controller	Dimensions	Phase/Polarization/ Control	Modulation/ Switching speed	Frequency range	Realized tunable functions	Ref.
DC voltage source	6 × 6 array	2-bit phase, single-pol., varactors	–	5 GHz	Beam scanning over a 100° × 100° window	[176]
Microcontroller	14 × 16 array	1-bit phase, single-pol., relay switches	–	60 GHz	Establishment of a robust link between transceivers by beam steering	[177]
FPGA	24 × 32 array	2-bit phase, single-pol., PIN diodes	–	3.2 GHz	Real-time reprogrammable digital-metasurface imager	[59]
FPGA	30 × 30 array	2-bit phase, single-pol., PIN diodes	–	9 GHz	Self-adaptive adjustment of EM radiation beams, single- and multi-beam steering	[85]
FPGA	16 × 16 array	2-bit phase, single-pol., varactors	78.125 kHz	3.6 GHz	Harmonic manipulation and BFSK wireless communication system	[115]
FPGA	768 elements	1-bit phase, single-pol., PIN diodes	500 kHz	2.4 GHz	Backscatter wireless communication with commodity Wi-Fi signals	[178]
FPGA	16 × 16 array	2-bit phase, dual-pol., PIN diodes	–	2.3 GHz, 28.5 GHz	Reflect antennas for beam scanning at 2.3 GHz & 28.5 GHz	[175]
Raspberry Pi controller	3200 elements	1-bit amplitude, single-pol., RF switch	1 MHz	2.4 GHz	Improvement of the signal strength and channel capacity for indoor wireless communication	[179]
FPGA	20 × 20 array	1-bit phase, dual-pol., PIN diodes	100 kHz	27.5–29.5 GHz	Beamforming both in the near field and far field	[82]
FPGA	576 elements	2-bit phase, single-pol., PIN diodes	–	2.55 GHz	Improvement of the quality of indoor wireless communication	[180]
FPGA	16 × 8 array	2-bit phase, single-pol., PIN diodes	2.5 MHz	9.5 GHz	Space- and frequency-division multiplexing for dual-channel wireless communication	[181]
DC voltage	10 × 10 array	3-bit phase, single-pol., varactors	–	3.15 GHz	Angle-insensitive beam steering	[131]
Voltage bias	50 × 50 cm^2	PZT actuators	–	27.2–28.2 GHz	Dynamic lens switching between single focus and dual focus	[182]
FPGA	56 × 20 array	1-bit phase, single-pol., PIN diodes	1.875 MHz	22–33 GHz	Broadband manipulation of harmonics for 256 QAM wireless communication	[116]
FPGA	20 × 20 array	1-bit phase, single-pol., PIN diodes	–	6.23 GHz	Dynamic beam scanning via reflection, transmission, or both	[171]
FPGA	20 × 20 array	1-bit phase, dual-pol., PIN diodes	–	6.9–7.7 GHz	Dual-polarized wide-angle beam-scanning up to ± 40°	[40]
FPGA	16 × 16 array	2-bit phase, single-pol., PIN diodes	–	25–28.6 GHz	Transmissive RIS with a high data rate, 2D beamforming up to ± 60°	[183]
Microcontroller	120 × 120 cm^2	3-bit phase, single-pol., varactors	–	3.5 GHz	Improvement of indoor wireless communication	[184]
Microcontroller	112 × 112 mm^2	1-bit phase, dual-pol., gear system	~ 4 s	32–36 GHz	Improvement of indoor 5G millimeter-wave wireless communication	[185]

lished that can assist information sensing, analog computing, and wireless communication [187]. With optimal control of the signal transmitter and terminal receiver, RIS-assisted wireless systems will become more flexible to support diverse user requirements, e.g., enhanced data rate, extended coverage, minimized power consumption, and more secure transmissions [87], [188], [189].

An RIS system needs to have sufficient physical size to compensate for the link budget deficit that results from its nearly passive implementation without any power amplification. In general, at least hundreds of elements must be equipped in an RIS system to offer a competitive gain. To realize affordable RIS implementation and deployment, each element needs to be low cost. The meta-atoms in an RIS need to have consistent phase and amplitude responses under external bias control and moderate angle stability under oblique incidence so that a single RIS can be used to serve different terminals at different locations.

In the following, we will give a comprehensive design example of a practical reflective RIS system and showcase its real application in enhancing the signal coverage of a wireless network. For practical considerations, a reflective-type reconfigurable metasurface is chosen in the RIS system due to its achievable high efficiency. Both 1-bit and 2-bit phase states are realized by loading PIN diodes into the EM resonant structure in the meta-atoms [180]. As illustrated in Figure 5(a), a simple H-shaped metallic structure backed by another metallic strip forms a capacitively coupled EM resonator under illumination of a *y*-polarized wave. A slot is cut in the middle strip and connected to a PIN diode, and a third layer of metallic sheet is used as a ground plane to block the EM wave for reflection operation. By switching on and off the PIN diode through DC voltage biasing, the resonance will be perturbed with a 180° reflection phase change, enabling a 1-bit reflective meta-atom. Such a design of a double-layer resonator ensures that most induced currents are distributed in the top metallic layer, which ensures a low-loss reflection mode for the meta-atom. The geometric structure is optimized to function as a 1-bit phase switchable reflector at a center frequency of approximately 2.55 GHz suitable for the 5G wireless network. Figures 5(b) and (c) show the simulated reflection phases and magnitudes of the designed meta-atom. By applying diverse bias voltages, a reflection phase change of approximately 180° and a high magnitude efficiency of over 80% are successfully achieved at 2.55 GHz.

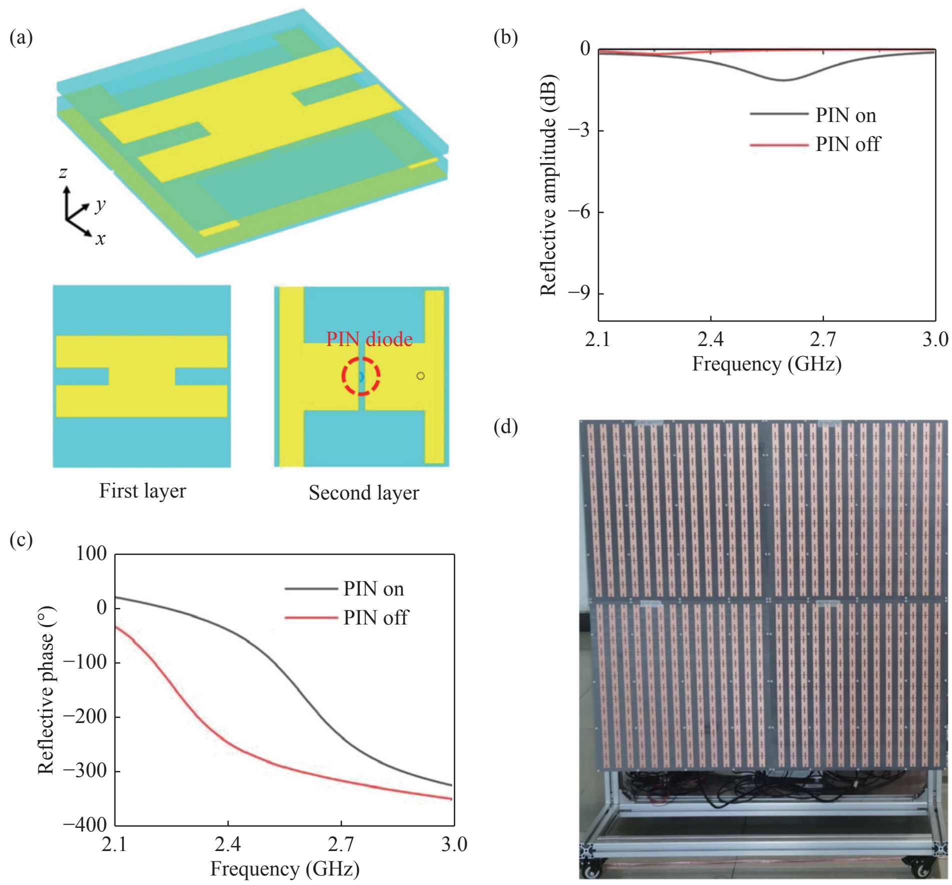

Figure 5 RIS realized with a 1-bit reflective metasurface. (a) Schematic of the meta-atom; Simulated (b) reflection amplitudes and (c) phases of the meta-atom; (d) Realized RIS system.

A single metasurface is designed with 14 × 14 meta-atoms with a size of 470 × 470 mm^2, and several metasurface sheets can be easily assembled together to realize different sized RIS boards required for practical deployment, as shown in Figure 5(d). To control the PIN diode in each meta-atom, we connect an off-surface control unit to the backside of the RIS board via ribbon cables with on-surface biasing lines, which altogether comprise the entire control circuit network. The phase state of each meta-atom is controlled through the bias network with FPGAs by enacting different binary coding sequences in a wireless remote manner through regular Wi-Fi signals, facilitating movable deployment of the RIS boards.

To demonstrate the ability to enhance the wireless signals in a weak coverage area, the RIS system can be operated to redistribute the EM wave channels from the transmitter to the receiver. To this aim, the RIS system controller uses signal intensity measurements from the local endpoints to maximize the signal strength at a particular location, which is realized through an optimization procedure employing the strengthen elitist genetic algorithm (SEGA) [190]. In the optimization process, different coding sequences are evaluated to create dynamic irregular beam shaping via the RIS to increase the signal intensity at the receiver based on the feedback from the measured power levels of the endpoints.

We have evaluated the RIS system in various indoor field tests. As an example, as shown in Figure 6, the RIS system is deployed in an indoor scenario including a corridor, interior walls, windows, and a large metallic door (blue rectangle in Figure 6. In the test, a signal transmitter working at 2.55 GHz is located at one end of the long corridor, and due to blocking of the EM waves by the metal door, weak coverage of the wireless signal is observed in the lower left corner at the other end of the corridor (denoted by the yellow dashed circle in Figure 6(a)). The wireless power intensity distribution in the corner is measured at 20 different locations using an omnidirectional dipole antenna, and the resulting signal coverage maps with and without deployment of the RIS system are compared, as shown in Figures 6(a)–(c). To enhance the signal coverage, two RIS boards, each with 2 × 3 metasurface sheets assembled in a movable frame, are deployed along the wall at the other end of the corridor, and different allocations of the RIS boards are studied. As shown in Figure 6(b), when two RIS boards are deployed together at the other side approximately 7.78 m from the emitter, the signal intensity can be significantly increased, with an average enhancement of more than 20 dB (a maximum of 33 dB) for the weak coverage area (in the left corner). We also consider the scenario in which the two RIS boards are located at different places, such as face to face at the two sides of the corner area, as shown in Figure 6(c). Although the RIS deployment is changed, similar wireless signal coverage to that in Figure 6(b) can be obtained with the beam forming ability through the two RIS boards, indicating that the influences of the RIS deployment positions can be largely eliminated by optimization of the irregular beam shaping. We also note that although the original signal strengths are quite nonuniform, with a power level difference of more than 30 dB (as shown in Figure 6(a)), by enacting RIS-assisted beam forming, a much more uniform signal power distribution can be obtained in the weak coverage area through adaptive coding pattern optimization (as shown in Figures 6(b) and (c)). Since higher received signals can lead to better signal-to-noise ratio performance and reduce communication failure, the RIS system is considered a promising technology able to improve the quality of next-generation wireless communication.

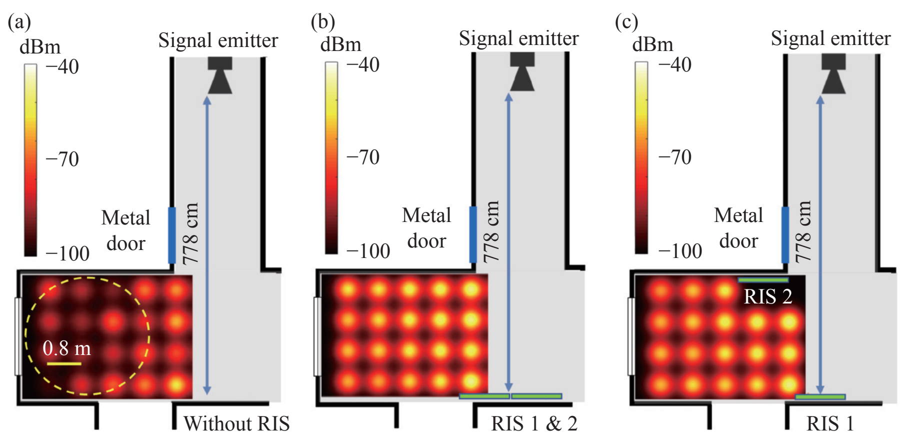

Figure 6 Indoor scenario and signal coverage enhancement with the deployment of a practical RIS system. Wireless signal intensity distributions (a) without and (b) and (c) with the RIS system (denoted by the green bars).

3. Full-space intelligent omni-metasurfaces

Most of the currently utilized RIS systems only support the reflection mode, implying that only backward scattering is modulated and access points on the opposite side of RISs are outside of wireless coverage. In addition to assisting indoor wireless communication via reflective RISs, improving outdoor-to-indoor or adjacent room communication by enhancing through-wall signals is similarly crucial. In such scenarios, RIS systems operating in transmission mode must provide flexible control of forward scattering, thus extending wireless coverage. For example, a passive metalens has been proposed to focus incoming waves to the other side of a wall with high efficiency, which can reconnect a network channel that is otherwise broken due to the weak signal strength [191]. Moreover, through-wall imaging using a dynamic metasurface antenna can be constructed by forming diverse radiation patterns scattered by the wall [111].

Despite the significant progress made for reflective and transmissive RISs, they may still suffer from the restriction that they cannot serve user terminals located on both sides of metasurfaces. To surmount this obstacle, omni-metasurfaces with full-space wireless coverage have been proposed to simultaneously serve the terminals on both sides of the RISs [105]. Although there have been a few attempts to assist wireless communication with omni-metasurfaces [179], [182], they only support dynamic control of either the reflection or transmission operation mode, which may further limit their scattering manipulation ability enacted by phase modulation.

Here, we present an intelligent omni-metasurface equipped with dynamic transmission/reflection phase control in different modes to further explore the possibilities of RISs in wireless communications. As illustrated in Figures 7(a)–(c), the proposed omni-metasurface can be flexibly switched among reflection mode, transmission mode, and duplex mode (simultaneous reflection and transmission) by modulating the loaded tunable components through an external hardware controller, thus customizing it for user terminals located on the same side, opposite sides and both sides of the surface. Moreover, by leveraging spatial coding profiles optimized by genetic algorithms, the proposed approach can overcome coverage holes and enhance local signals in both backward and forward half-spaces, resulting in full-space wireless coverage.

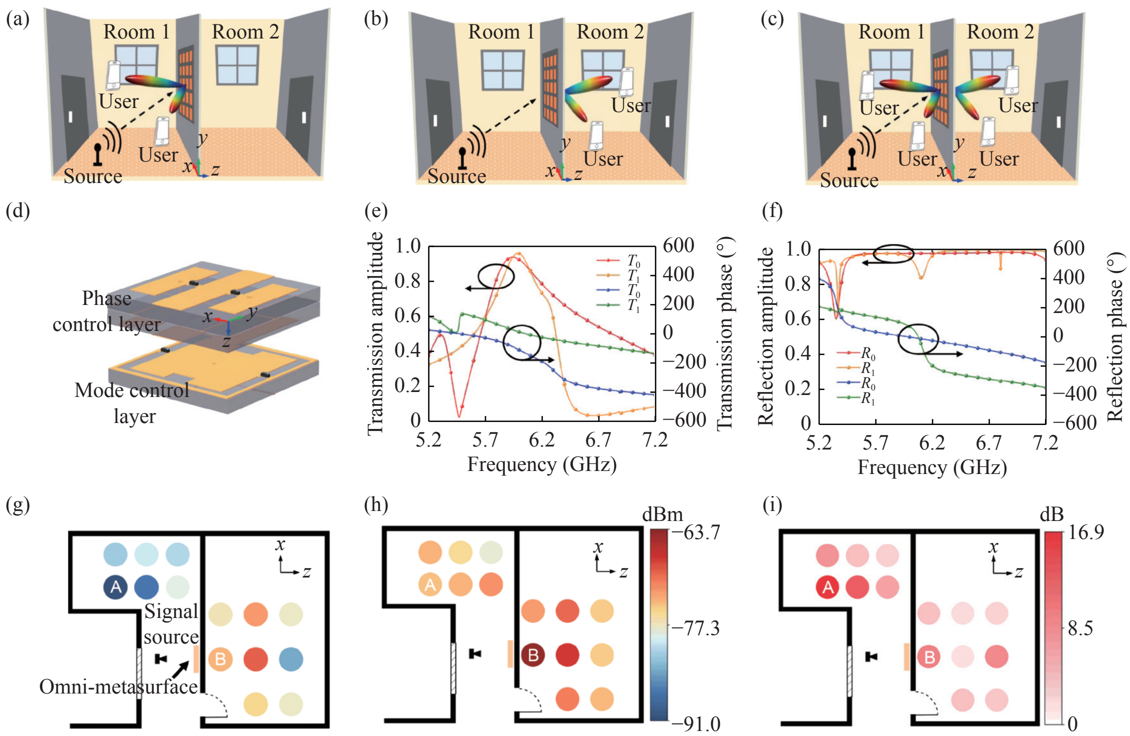

Figure 7 Proposed omni-metasurface for assisting full-space wireless communication. (a) Reflection mode; (b) Transmission mode; (c) Duplex mode; (d) Perspective view of the meta-atom; Simulated (e) transmission and (f) reflection performance of the proposed meta-atom; Measured signal strength (g) without and (h) with the omni-metasurface; (i) Measured signal strength enhancement.

As illustrated in Figure 7(d), the key procedure to achieve an intelligent omni-metasurface is simplified by separately designing two distinct meta-structures capable of phase modulation and transmission-reflection control and then combining them to form the required meta-atom [171]. The phase-control layer is designed with a 180° phase difference for transmission waves by simultaneously switching on or off the embedded PIN diodes, and the corresponding operation state is encoded as “0” or “1”. Meanwhile, the transmission-reflection mode-control layer is designed with high-efficiency reflection or high-efficiency transmission when the inserted PIN diodes are switched to the “OFF” or “ON” state, and the corresponding operation state is encoded as “R” or “T”, respectively. Therefore, a 1-bit phase configuration in transmission operation mode can be directly acquired by switching diodes of the phase-control layer on or off and setting the mode-control layer to transmission mode. In contrast, a 1-bit phase configuration in reflection mode can be implemented by altering diodes of the phase-control layer on or off and setting the mode-control layer to reflection mode. The corresponding simulated results for the four operation states are shown in Figures 7(e) and (f), from which we can observe a 180° phase difference for both transmitted and reflected waves at 6.23 GHz.

To experimentally verify the full-space wave manipulation abilities of the design, a prototype consisting of 20 × 20 meta-atoms with a total size of 408 × 418 mm^2 is fabricated, which can be utilized to provide backward or forward wireless coverage by setting all the meta-atoms to reflection or transmission mode. Moreover, it can be utilized to extend the provided wireless coverage into full space by adopting a multiplexing technique and setting the meta-atoms to both reflection and transmission modes.

As an exemplary demonstration, the omni-metasurface is utilized to assist adjacent room communication by enhancing through-wall and reflected signals in a real-world scenario with windows, doors, and interior walls. The omni-metasurface is placed on a wall with a propagation loss of approximately −4.5 dB. An Alford-loop-type antenna with an omnidirectional radiation pattern for horizontal polarization is adopted to mimic a user terminal. Meanwhile, a horn antenna is adopted as the signal source and placed at a distance of 1.16 m from the metasurface. To investigate the ability to reshape wireless signals propagating in full space, we evaluate the signals received at 8 locations in the forward room and 6 locations in the backward room. Every receiver location in the forward room is separated by a distance of 1.36 m in the x-direction and 1.65 m in the z-

direction, and those in the backward room are separated by a distance of 1.2 m in both the *x*- and *z*-directions.

For each receiver location, we search for the spatial coding pattern that will maximize the received signal power. Specifically, based on a genetic algorithm and the real-time measured feedback signal strength, we configure test states of diodes loaded into the metasurface and monitor the changes in the received signal in real time. The power of the signal source is set to 0 dBm. The measured results without and with the omni-metasurface in the full space are plotted in Figures 7(g) and (h), respectively. The received signal at every position can be enhanced. For a clear view, the measured enhancement of the signal strength is displayed in Figure 7(i). In the backward room, the reflected signal can be enhanced by a maximum of 16.9 dB at position A and an average of 8.7 dB at all positions. In the forward room, the through-wall signal can be improved by up to 9.9 dB at most at position B and 4.7 dB on average at all positions. To simultaneously activate the reflection and transmission functions, a field or spatial multiplexing method is used in the design, assisted by an optimization algorithm, that is, part of the meta-atoms are switched to reflection mode while the others are switched to transmission mode based on the algorithm calculation. The reflected or transmitted beam width may be narrowed by the RISs, which will reduce the signal coverage. To solve this issue, a dynamic sensing technique (e.g., beam scanning) may be used to find the users' locations and then output on-demand solutions to enhance the wireless signal intensity. Notably, signal enhancement is not only relevant to transmitters and receivers but also dependent on the propagation environment. Since stronger received signals can lead to better signal-to-noise ratio performance and reduce communication failure, the proposed omni-metasurface may be able to improve both indoor and outdoor-to-indoor communication quality. Further evolution of the omni-metasurface concept into a self-learning version by utilizing sensors is envisioned. In this way, such surfaces can actively adapt to different requirements without human interference. Meanwhile, more theoretical physics-based models are encouraged to guide the optimization of RIS-assisted wireless communication.

IV. Summary and Outlooks

In summary, we provide an overview of the RIS concept, focusing on the design in the microwave regime. The development of this field originated from metamaterials and metasurfaces. The design methods are similar between RISs and reconfigurable metasurfaces at the meta-atom level, both involving co-optimization of the resonant structure and the actively controllable component. We summarize the various control methods for reconfigurable metasurfaces, including current and voltage bias, mechanical actuation, and thermal driving. As practical demonstrations, we show our recent works indicating that RISs can dynamically reshape the EM propagation environment to achieve versatile wave functionalities such as local signal enhancement and dynamic beam shaping in reflection or full-space operations. Finally, we would like to mention some challenges in this emerging field and promising research directions based on our own perspectives.

The concept of RISs has gradually evolved from metamaterials and metasurfaces, so they have the advantages of these previous concepts but pose additional challenges for the design of bias networks and external controllers. At the physical level, RIS meta-atoms that have excellent EM performance with low-cost and low-complexity bias networks are desired. However, the control range of the phases and their quantization levels contradict the design of the bias network. For example, if varactors are used for RIS design to achieve continuously tunable phase responses in the microwave region, then a continuous change in the bias voltage should be adopted, but this will increase the complexity of the external voltage controller because a high-speed digital-to-analog converter and a voltage amplifier should be added to each bias line. Suppose that several PIN diodes are adopted to achieve a multibit RIS. In this case, each diode in a meta-atom should be independently addressed by the voltage controller through an independent bias line, increasing the design complexity. These problems will be more apparent for the high-frequency region, such as the 5G and 6G millimeter bands, where the physical space in the meta-atoms becomes more compacted. In addition, reconfigurable reflectarrays and transmitarrays can also perform tunable wave functionalities in many cases, although with a larger element size comparable to half of the wavelength. In general, reconfigurable reflectarrays and transmitarrays are used for tuning the incidence wave from a feed antenna, while RISs are mostly used for reshaping the wave in the far-field region of the antenna system or that reflected from the environment. However, the relevant concepts, especially from the viewpoint of constituent elements, have become vague in recent years, and the idea that the surfaces used in RIS systems should have tunability in shaping the EM wave propagation environment may become prevalent, regardless of their element types as metasurfaces, reflectarrays, or even frequency-selective surfaces based on the original definitions. Due to restrictions on paper length, we were not able to include all the branches of reconfigurable artificial structures and materials, for example, reflectarrays, transmitarrays, and the active frequency-selective surfaces [73]–[79], [192], [193].

High-speed control and response of RIS elements are necessary for fast modulation of the EM environment and wave propagation. Although stand-alone diodes have a very fast response time approaching several nanoseconds, the upper limit is restricted by the overall circuit loop, including the resonant structures, bias lines inside and outside the meta-atoms, and external controllers. Hence, the switching or control speed will be much slower in experiments. In addition, realizing high-efficiency RISs comparable to totally passive structures is still a great challenge because tunable materials or components will bring additional loss that cannot be ignored. Such energy loss would further cause unequal amplitude responses among different operating states of the meta-atoms. Therefore, new mechanisms involving coupling effects between materials and EM waves and new materials with low-loss characteristics should be explored to solve the above problems.

For system-level implementations, most of the reported RIS research is focused on tunable components without power amplification functions. In other words, the output wave energy is always less than the input. Due to the "multiplicative fading" effect introduced by RISs, achieving noticeable capacity gains is almost impossible for RISs without amplification in some cases where the direct link between the emitter and receiver is not weak, but recent studies have shown that active RISs with energy amplification can possibly overcome this effect [194]. The nonreciprocal and power-sensitive properties of chip amplifiers may influence the modulation signals and information transmission, which should be seriously considered for practical applications [195]–[197].

Most of the existing metasurfaces are designed for reflection operations, so they may have the disadvantages of a high profile and a blockage effect from the feeding/receiving antennas. Moreover, they cannot process transmitted waves when transmission manipulation is necessary, for example, in an indoor environment with several subrooms. Although recent studies have proposed several ways to implement omni-metasurfaces to tune EM waves in both reflection and transmission modes, there are still some problems that could be further resolved, such as the efficiency, bandwidth, and independently addressable properties.

The heuristic use of AI-empowered RIS applications has combined computation-enabled AI and physical metastructures, accelerating RIS development toward smart platforms. Most AI-empowered RISs are developed for one or several kinds of problems based on a vast amount of training data, so how to extend the generalization of AI-empowered RISs so that they can adapt well to unexpected tasks may be further explored. In addition, the metasurface and the training data are separated at the physical level in most current strategies to execute deep-learning methods. Data training and learning directly executed by the metasurface itself may maximally alleviate the human intervention and accelerate the response time.

RISs provide a new paradigm in wireless communications, but the realization of RISs is still in its early stages and far from widespread use in the real world [198]. Standardization work should be done at a regional level for industrial and commercial services. Although extensive research and activities are dedicated to RISs globally, standardization work is still in progress. RISs should be large enough to capture incident waves and thus offer a competitive gain, especially for outdoor environments. Therefore, to enable flexible deployment of an RIS, which may contain hundreds or thousands of elements, the RIS elements should be fabricated at a low cost, and the external control signals should be realized with low power consumption and low complexity. In addition, RISs may work jointly with multiantenna base stations and receiving terminals, increasing the optimization algorithm complexity. Outdoor applications will even impose additional requirements to withstand possibly harsh environments, such as wind, rain, snow, sunlight, temperature fluctuations, and dust. This also requires that the RIS, control system, and EM properties should be stable for months or years. Reshaping of the EM propagation environment in a particular communication band for practical use with minimum influence on other wireless bands is desired. However, RISs have difficulty discriminating or even cannot discriminate the frequency symbols of signals with high accuracy because RISs do not have digital or RF chains to process incident signals.

RISs capable of dynamically reshaping EM waves are the physical basis for further use in wireless communication, while studies beyond the physical layer are a key step to make RISs truly applicable. This review mainly focuses on the design methods and practical demonstrations of EM wave enhancement. However, from the viewpoint of wireless communication theory, there are still many challenges and problems, such as energy-efficient communication channel sensing and estimation, practical protocols for information exchange, and real-time allocation and optimization of different RISs to serve multiple data streams in dynamic and heterogeneous networks. More concrete discussions from the viewpoint of wireless communication theory can be found in some recent reviews [90], [199], [200]. Overall, the two communities need more synergic research and dialog to push this work further for real-world applications. Nevertheless, the rapid development of this field may somehow overcome these issues in the near future, making RIS technologies truly intelligent platforms.

Acknowledgements

This work was supported by the National Natural Science Foundation of China (Grant Nos. 62271243, 62071215, 91963128, and 61731010), the National Key Research and Development Program of China (Grant No. 2017YFA0700201), and the Joint Fund of Ministry of Education for Equipment Pre-research (Grant No. 8091B032112). We would like to acknowledge the support from the Priority Academic Program Development of Jiangsu Higher Education Institutions (PAPD), Fundamental Research Funds for the Central Universities, and Jiangsu Provincial Key Laboratory of Advanced Manipulating Technique of Electromagnetic Wave.

References

[1] R. A. Shelby, D. R. Smith, and S. Schultz, "Experimental verification of a negative index of refraction," *Science*, vol. 292, no. 5514, pp. 77–79, 2001.

[2] D. Schurig, J. J. Mock, B. J. Justice, *et al*., "Metamaterial electromagnetic cloak at microwave frequencies," *Science*, vol. 314, no. 5801, pp. 977–980, 2006.

[3] J. B. Pendry, "Negative refraction makes a perfect lens," *Physical Review Letters*, vol. 85, no. 18, pp. 3966–3969, 2000.

[4] N. I. Landy, S. Sajuyigbe, J. J. Mock, *et al*., "Perfect metamaterial absorber," *Physical Review Letters*, vol. 100, no. 20, article no. 207402, 2008.

[5] K. Chen, G. W. Ding, G. W. Hu, *et al*., "Directional Janus metasurface," *Advanced Materials*, vol. 32, no. 2, article no. 1906352, 2020.

[6] Q. He, S. L. Sun, S. Y. Xiao, *et al*., "High-efficiency metasurfaces: Principles, realizations, and applications," *Advanced Optical Materials*, vol. 6, no. 19, article no. 1800415, 2018.

[7] O. Quevedo-Teruel, H. S. Chen, A. Díaz-Rubio, *et al*., "Roadmap on metasurfaces," *Journal of Optics*, vol. 21, no. 7, article no. 073002, 2019.

[8] K. Chen and Y. J. Feng, "A review of recent progress on directional metasurfaces: Concept, design, and application," *Journal of Physics D: Applied Physics*, vol. 55, no. 38, article no. 383001, 2022.

[9] N. F. Yu and F. Capasso, "Flat optics with designer metasurfaces," *Nature Materials*, vol. 13, no. 2, pp. 139–150, 2014.

[10] S. B. Glybovski, S. A. Tretyakov, P. A. Belov, *et al*., "Metasurfaces: From microwaves to visible," *Physics Reports*, vol. 634, pp. 1–72, 2016.

[11] T. J. Cui, S. Liu, and L. Zhang, "Information metamaterials and metasurfaces," *Journal of Materials Chemistry C*, vol. 5, no. 15, pp. 3644–3668, 2017.

[12] N. F. Yu, P. Genevet, M. A. Kats, *et al*., "Light propagation with phase discontinuities: Generalized laws of reflection and refraction," *Science*, vol. 334, no. 6054, pp. 333–337, 2011.

[13] S. L. Sun, Q. He, S. Y. Xiao, *et al*., "Gradient-index meta-surfaces as a bridge linking propagating waves and surface waves," *Nature Materials*, vol. 11, no. 5, pp. 426–431, 2012.

[14] E. Arbabi, S. M. Kamali, A. Arbabi, *et al*., "Full-stokes imaging polarimetry using dielectric metasurfaces," *ACS Photonics*, vol. 5, no. 8, pp. 3132–3140, 2018.

[15] X. J. Ni, A. V. Kildishev, and V. M. Shalaev, "Metasurface holograms for visible light," *Nature Communications*, vol. 4, no. 1, article no. 2807, 2013.

[16] L. L. Huang, X. Z. Chen, H. Mühlenbernd, *et al*., "Three-dimensional optical holography using a plasmonic metasurface," *Nature Communications*, vol. 4, no. 1, article no. 2808, 2013.

[17] X. J. Ni, Z. J. Wong, M. Mrejen, *et al*., "An ultrathin invisibility skin cloak for visible light," *Science*, vol. 349, no. 6254, pp. 1310–1314, 2015.

[18] X. Wan, X. P. Shen, Y. Luo, *et al*., "Planar bifunctional Luneburg-fisheye lens made of an anisotropic metasurface," *Laser & Photonics Reviews*, vol. 8, no. 5, pp. 757–765, 2014.

[19] F. Aieta, P. Genevet, M. A. Kats, *et al*., "Aberration-free ultrathin flat lenses and axicons at telecom wavelengths based on plasmonic metasurfaces," *Nano Letters*, vol. 12, no. 9, pp. 4932–4936, 2012.

[20] W. T. Chen, A. Y. Zhu, V. Sanjeev, *et al*., "A broadband achromatic metalens for focusing and imaging in the visible," *Nature Nanotechnology*, vol. 13, no. 3, pp. 220–226, 2018.

[21] M. Khorasaninejad, W. T. Chen, R. C. Devlin, *et al*., "Metalenses at visible wavelengths: Diffraction-limited focusing and subwavelength resolution imaging," *Science*, vol. 352, no. 6290, pp. 1190–1194, 2016.

[22] K. Zhang, Y. Y. Yuan, X. M. Ding, *et al*., "Polarization-engineered noninterleaved metasurface for integer and fractional orbital angular momentum multiplexing," *Laser & Photonics Reviews*, vol. 15, no. 1, article no. 2000351, 2021.

[23] G. W. Ding, K. Chen, X. Y. Luo, *et al*., "Dual-helicity decoupled coding metasurface for independent spin-to-orbital angular momentum conversion," *Physical Review Applied*, vol. 11, no. 4, article no. 044043, 2019.

[24] W. L. Guo, K. Chen, G. M. Wang, *et al*., "Transmission–reflection-selective metasurface and its application to RCS reduction of high-gain reflector antenna," *IEEE Transactions on Antennas and Propagation*, vol. 68, no. 3, pp. 1426–1435, 2020.

[25] S. Liu, T. J. Cui, Q. Xu, *et al*., "Anisotropic coding metamaterials and their powerful manipulation of differently polarized terahertz waves," *Light: Science & Applications*, vol. 5, no. 5, article no. e16076, 2016.

[26] L. Cui, W. J. Wang, G. W. Ding, *et al*., "Polarization-dependent bi-functional metasurface for directive radiation and diffusion-like scattering," *AIP Advances*, vol. 7, no. 11, article no. 115214, 2017.

[27] M. Khorasaninejad, W. T. Chen, A. Y. Zhu, *et al*., "Multispectral chiral imaging with a metalens," *Nano Letters*, vol. 16, no. 7, pp. 4595–4600, 2016.

[28] B. Sima, K. Chen, X. Y. Luo, *et al*., "Combining frequency-selective scattering and specular reflection through phase-dispersion tailoring of a metasurface," *Physical Review Applied*, vol. 10, no. 6, article no. 064043, 2018.

[29] X. Y. Luo, W. L. Guo, K. Qu, *et al*., "Quad-channel independent wavefront encoding with dual-band multitasking metasurface," *Optics Express*, vol. 29, no. 10, pp. 15678–15688, 2021.

[30] C. W. Wan, C. J. Dai, S. Wan, *et al*., "Dual-encryption freedom via a monolayer-nanotextured Janus metasurface in the broadband visible," *Optics Express*, vol. 29, no. 21, pp. 33954–33961, 2021.

[31] H. X. Xu, C. H. Wang, G. W. Hu, *et al*., "Spin-encoded wavelength-direction multitasking Janus metasurfaces," *Advanced Optical Materials*, vol. 9, no. 11, article no. 2100190, 2021.

[32] T. J. Cui, M. Q. Qi, X. Wan, *et al*., "Coding metamaterials, digital metamaterials and programmable metamaterials," *Light: Science & Applications*, vol. 3, no. 10, article no. e218, 2014.

[33] Z. Q. Miao, Q. Wu, X. Li, *et al*., "Widely tunable terahertz phase modulation with gate-controlled graphene metasurfaces," *Physical Review X*, vol. 5, no. 4, article no. 041027, 2015.

[34] S. Lee, W. T. Kim, J. H. Kang, *et al*., "Single-layer metasurfaces as spectrally tunable terahertz half- and quarter-waveplates," *ACS Applied Materials & Interfaces*, vol. 11, no. 8, pp. 7655–7660, 2019.

[35] J. Y. Guo, T. Wang, H. Zhao, *et al*., "Reconfigurable terahertz metasurface pure phase holograms," *Advanced Optical Materials*, vol. 7, no. 10, article no. 1801696, 2019.

[36] M. Y. Shalaginov, S. S. An, Y. F. Zhang, *et al*., "Reconfigurable all-dielectric metalens with diffraction-limited performance," *Nature Communications*, vol. 12, no. 1, article no. 1225, 2021.

[37] G. Y. Qu, W. H. Yang, Q. H. Song, *et al*., "Reprogrammable metahologram for optical encryption," *Nature Communications*, vol. 11, no. 1, article no. 5484, 2020.

[38] C. Huang, B. Sun, W. B. Pan, *et al*., "Dynamical beam manipulation based on 2-bit digitally-controlled coding metasurface," *Scientific Reports*, vol. 7, article no. 42302, 2017.

[39] X. Y. Luo, W. L. Guo, K. Chen, *et al*., "Active cylindrical metasurface with spatial reconfigurability for tunable backward scattering reduction," *IEEE Transactions on Antennas and Propagation*, vol. 69, no. 6, pp. 3332–3340, 2021.

[40] N. Zhang, K. Chen, J. M. Zhao, *et al*., "A dual-polarized reconfigurable reflectarray antenna based on dual-channel programmable metasurface," *IEEE Transactions on Antennas and Propagation*, vol. 70, no. 9, pp. 7403–7412, 2022.

[41] L. L. Li, T. Jun Cui, W. Ji, *et al*., "Electromagnetic reprogrammable coding-metasurface holograms," *Nature Communications*, vol. 8, no. 1, article no. 197, 2017.

[42] M. F. Imani, T. Sleasman, and D. R. Smith, "Two-dimensional dynamic metasurface apertures for computational microwave imaging," *IEEE Antennas and Wireless Propagation Letters*, vol. 17, no. 12, pp. 2299–2303, 2018.

[43] J. Zhang, X. Z. Wei, I. D. Rukhlenko, *et al*., "Electrically tunable metasurface with independent frequency and amplitude modulations," *ACS Photonics*, vol. 7, no. 1, pp. 265–271, 2020.

[44] H. Chen, Z. G. Liu, W. B. Lu, *et al*., "Full polarization transformation using graphene in microwave frequencies," *IEEE Transactions on Antennas and Propagation*, vol. 68, no. 5, pp. 3760–3769,

2020.

[45] O. Buchnev, N. Podoliak, M. Kaczmarek, *et al*., "Electrically controlled nanostructured metasurface loaded with liquid crystal: Toward multifunctional photonic switch," *Advanced Optical Materials*, vol. 3, no. 5, pp. 674–679, 2015.

[46] A. Komar, R. Paniagua-Domínguez, A. Miroshnichenko, *et al*., "Dynamic beam switching by liquid crystal tunable dielectric metasurfaces," *ACS Photonics*, vol. 5, no. 5, pp. 1742–1748, 2018.

[47] M. Decker, C. Kremers, A. Minovich, *et al*., "Electro-optical switching by liquid-crystal controlled metasurfaces," *Optics Express*, vol. 21, no. 7, pp. 8879–8885, 2013.

[48] J. B. Wu, Z. Shen, S. J. Ge, *et al*., "Liquid crystal programmable metasurface for terahertz beam steering," *Applied Physics Letters*, vol. 116, no. 13, article no. 131104, 2020.

[49] B. W. Chen, X. R. Wang, W. L. Li, *et al*., "Electrically addressable integrated intelligent terahertz metasurface," *Science Advances*, vol. 8, no. 41, article no. eadd1296, 2022.

[50] E. Takou, A. C. Tasolamprou, O. Tsilipakos, *et al*., "Anapole tolerance to dissipation losses in thermally tunable water-based metasurfaces," *Physical Review Applied*, vol. 15, no. 1, article no. 014043, 2021.

[51] A. E. Cardin, S. R. Silva, S. R. Vardeny, *et al*., "Surface-wave-assisted nonreciprocity in spatio-temporally modulated metasurfaces," *Nature Communications*, vol. 11, no. 1, article no. 1469, 2020.

[52] W. X. Yang, K. Chen, Y. L. Zheng, *et al*., "Angular-adaptive reconfigurable spin-locked metasurface retroreflector," *Advanced Science*, vol. 8, no. 21, article no. 2100885, 2021.

[53] Y. L. Zheng, K. Chen, W. X. Yang, *et al*., "Kirigami reconfigurable gradient metasurface," *Advanced Functional Materials*, vol. 32, no. 5, article no. 2107699, 2022.

[54] E. Arbabi, A. Arbabi, S. M. Kamali, *et al*., "MEMS-tunable dielectric metasurface lens," *Nature Communications*, vol. 9, no. 1, article no. 812, 2018.

[55] I. V. Shadrivov, P. V. Kapitano.a, S. I. Maslovski, *et al*., "Metamaterials controlled with light," *Physical Review Letters*, vol. 109, no. 8, article no. 083902, 2012.

[56] X. G. Zhang, W. X. Jiang, H. L. Jiang, *et al*., "An optically driven digital metasurface for programming electromagnetic functions," *Nature Electronics*, vol. 3, no. 3, pp. 165–171, 2020.

[57] L. Chen, Q. F. Nie, Y. Ruan, *et al*., "Light-controllable metasurface for microwave wavefront manipulation," *Optics Express*, vol. 28, no. 13, pp. 18742–18749, 2020.

[58] X. Y. Duan, S. Kamin, and N. Liu, "Dynamic plasmonic colour display," *Nature Communications*, vol. 8, article no. 14606, 2017.

[59] L. L. Li, H. X. Ruan, C. Liu, *et al*., "Machine-learning reprogrammable metasurface imager," *Nature Communications*, vol. 10, no. 1, article no. 1082, 2019.

[60] H. H. Yang, X. Y. Cao, F. Yang, *et al*., "A programmable metasurface with dynamic polarization, scattering and focusing control," *Scientific Reports*, vol. 6, article no. 35692, 2016.

[61] K. Chen, N. Zhang, G. W. Ding, *et al*., "Active anisotropic coding metasurface with independent real-time reconfigurability for dual polarized waves," *Advanced Materials Technologies*, vol. 5, no. 2, article no. 1900930, 2020.

[62] L. Zhang, X. Q. Chen, S. Liu, *et al*., "Space-time-coding digital metasurfaces," *Nature Communications*, vol. 9, no. 1, article no. 4334, 2018.

[63] N. Zhang, K. Chen, Q. Hu, *et al*., "Spatiotemporal metasurface to control electromagnetic wave scattering," *Physical Review Applied*, vol. 17, no. 5, article no. 054001, 2022.

[64] X. D. Bai, F. W. Kong, Y. T. Sun, *et al*., "High-efficiency transmissive programmable metasurface for multimode OAM generation," *Advanced Optical Materials*, vol. 8, no. 17, article no. 2000570, 2020.

[65] Y. Wang, S. H. Xu, F. Yang, *et al*., "1 bit dual-linear polarized reconfigurable Transmitarray antenna using asymmetric dipole elements with parasitic bypass dipoles," *IEEE Transactions on Antennas and Propagation*, vol. 69, no. 2, pp. 1188–1192, 2021.

[66] L. Boccia, I. Russo, G. Amendola, *et al*., "Multilayer antenna-filter antenna for beam-steering transmit-array applications," *IEEE Transactions on Microwave Theory and Techniques*, vol. 60, no. 7, pp. 2287–2300, 2012.

[67] J. Y. Lau and S. V. Hum, "A planar reconfigurable aperture with lens and reflectarray modes of operation," *IEEE Transactions on Microwave Theory and Techniques*, vol. 58, no. 12, pp. 3547–3555, 2010.

[68] Q. Hu, K. Chen, N. Zhang, *et al*., "Arbitrary and dynamic poincaré sphere polarization converter with a time-varying metasurface," *Advanced Optical Materials*, vol. 10, no. 4, article no. 2101915, 2022.

[69] C. Huang, C. L. Zhang, J. N. Yang, *et al*., "Reconfigurable metasurface for multifunctional control of electromagnetic waves," *Advanced Optical Materials*, vol. 5, no. 22, article no. 1700485, 2017.

[70] Z. N. Wu, Y. Ra'di, and A. Grbic, "Tunable metasurfaces: A polarization rotator design," *Physical Review X*, vol. 9, no. 1, article no. 011036, 2019.

[71] W. Li, S. Xia, B. He, *et al*., "A reconfigurable polarization converter using active metasurface and its application in horn antenna," *IEEE Transactions on Antennas and Propagation*, vol. 64, no. 12, pp. 5281–5290, 2016.

[72] Q. Hu, K. Chen, J. M. Zhao, *et al*., "On-demand dynamic polarization meta-transformer," *Laser & Photonics Reviews*, vol. 17, no. 1, article no. 2200479, 2023.

[73] M. Riel and J. J. Laurin, "Design of an electronically beam scanning reflectarray using aperture-coupled elements," *IEEE Transactions on Antennas and Propagation*, vol. 55, no. 5, pp. 1260–1266, 2007.

[74] A. Clemente, L. Dussopt, R. Sauleau, *et al*., "Wideband 400-element electronically reconfigurable transmitarray in X band," *IEEE Transactions on Antennas and Propagation*, vol. 61, no. 10, pp. 5017–5027, 2013.

[75] J. Q. Han, L. Li, G. Y. Liu, *et al*., "A wideband 1 bit 12 × 12 reconfigurable beam-scanning reflectarray: Design, fabrication, and measurement," *IEEE Antennas and Wireless Propagation Letters*, vol. 18, no. 6, pp. 1268–1272, 2019.

[76] L. Z. Song, P. Y. Qin, H. Zhu, *et al*., "Wideband conformal transmitarrays for E-band multi-beam applications," *IEEE Transactions on Antennas and Propagation*, vol. 70, no. 11, pp. 10417–10425, 2022.

[77] X. Wang, P. Y. Qin, A. Tuyen Le, *et al*., "Beam scanning transmitarray employing reconfigurable dual-layer Huygens element," *IEEE Transactions on Antennas and Propagation*, vol. 70, no. 9, pp. 7491–7500, 2022.

[78] L. Dussopt, A. Moknache, J. Saily, *et al*., "A V-band switched-beam linearly polarized transmit-array antenna for wireless backhaul applications," *IEEE Transactions on Antennas and Propagation*, vol. 65, no. 12, pp. 6788–6793, 2017.

[79] M. Yi, Y. Bae, S. Yoo, *et al*., "Digitized reconfigurable metal Reflectarray surfaces for millimeter-wave beam-engineering," *Applied Sciences*, vol. 11, no. 13, article no. 5811, 2021.

[80] O. Tsilipakos, A. C. Tasolamprou, A. Pitilakis, *et al*., "Toward intelligent metasurfaces: The progress from globally tunable metasurfaces to software-defined metasurfaces with an embedded network of controllers," *Advanced Optical Materials*, vol. 8, no. 17, article no. 2000783, 2020.

[81] H. P. Wang, Y. B. Li, H. Li, *et al*., "Intelligent metasurface with frequency recognition for adaptive manipulation of electromagnetic wave," *Nanophotonics*, vol. 11, no. 7, pp. 1401–1411, 2022.

[82] J. B. Gros, V. Popov, M. A. Odit, *et al*., "A reconfigurable intelligent surface at mmWave based on a binary phase tunable metasurface," *IEEE Open Journal of the Communications Society*, vol. 2, pp. 1055–1064, 2021.

[83] H. H. Yang, F. Yang, X. Y. Cao, *et al*., "A 1600-element dual-frequency electronically reconfigurable reflectarray at X/Ku-band,"

IEEE Transactions on Antennas and Propagation, vol. 65, no. 6, pp. 3024–3032, 2017.
[84] H. Lin, W. Yu, R. X. Tang, *et al*., "A dual-band reconfigurable intelligent metasurface with beam steering," *Journal of Physics D: Applied Physics*, vol. 55, no. 24, article no. 245002, 2022.
[85] Q. Ma, G. D. Bai, H. B. Jing, *et al*., "Smart metasurface with self-adaptively reprogrammable functions," *Light: Science & Applications*, vol. 8, article no. 98, 2019.
[86] J. Y. Liu, Y. P. Duan, T. Zhang, *et al*., "Dual-polarized and real-time reconfigurable metasurface absorber with infrared-coded remote-control system," *Nano Research*, vol. 15, no. 8, pp. 7498–7505, 2022.
[87] E. Basar, M. D. Renzo, J. De Rosny, *et al*., "Wireless communications through reconfigurable intelligent surfaces," *IEEE Access*, vol. 7, pp. 116753–116773, 2019.
[88] Q. Q. Wu and R. Zhang, "Towards smart and reconfigurable environment: Intelligent reflecting surface aided wireless network," *IEEE Communications Magazine*, vol. 58, no. 1, pp. 106–112, 2020.
[89] J. Z. Hu, H. L. Zhang, B. Y. Di, *et al*., "Reconfigurable intelligent surface based RF sensing: Design, optimization, and implementation," *IEEE Journal on Selected Areas in Communications*, vol. 38, no. 11, pp. 2700–2716, 2020.
[90] M. Di Renzo, A. Zappone, M. Debbah, *et al*., "Smart radio environments empowered by reconfigurable intelligent surfaces: How it works, state of research, and the road ahead," *IEEE Journal on Selected Areas in Communications*, vol. 38, no. 11, pp. 2450–2525, 2020.
[91] M. A. ElMossallamy, H. L. Zhang, L. Y. Song, *et al*., "Reconfigurable intelligent surfaces for wireless communications: Principles, challenges, and opportunities," *IEEE Transactions on Cognitive Communications and Networking*, vol. 6, no. 3, pp. 990–1002, 2020.
[92] J. Y. Dai, W. K. Tang, M. Z. Chen, *et al*., "Wireless communication based on information metasurfaces," *IEEE Transactions on Microwave Theory and Techniques*, vol. 69, no. 3, pp. 1493–1510, 2021.
[93] C. Liaskos, S. Nie, A. Tsioliaridou, *et al*., "A new wireless communication paradigm through software-controlled metasurfaces," *IEEE Communications Magazine*, vol. 56, no. 9, pp. 162–169, 2018.
[94] S. W. Zhang and R. Zhang, "Capacity characterization for intelligent reflecting surface aided MIMO communication," *IEEE Journal on Selected Areas in Communications*, vol. 38, no. 8, pp. 1823–1838, 2020.
[95] X. D. Mu, Y. W. Liu, L. Guo, *et al*., "Capacity and optimal resource allocation for IRS-assisted multi-user communication systems," *IEEE Transactions on Communications*, vol. 69, no. 6, pp. 3771–3786, 2021.
[96] G. P. Wang, F. F. Gao, R. F. Fan, *et al*., "Ambient backscatter communication systems: Detection and performance analysis," *IEEE Transactions on Communications*, vol. 64, no. 11, pp. 4836–4846, 2016.
[97] L. Wei, C. W. Huang, G. C. Alexandropoulos, *et al*., "Channel estimation for RIS-empowered multi-user MISO wireless communications," *IEEE Transactions on Communications*, vol. 69, no. 6, pp. 4144–4157, 2021.
[98] S. Hu, F. Rusek, and O. Edfors, "Beyond massive MIMO: The potential of positioning with large intelligent surfaces," *IEEE Transactions on Signal Processing*, vol. 66, no. 7, pp. 1761–1774, 2018.
[99] S. Hu, F. Rusek, and O. Edfors, "Beyond massive MIMO: The potential of data transmission with large intelligent surfaces," *IEEE Transactions on Signal Processing*, vol. 66, no. 10, pp. 2746–2758, 2018.
[100] Y. Han, W. K. Tang, S. Jin, *et al*., "Large intelligent surface-assisted wireless communication exploiting statistical CSI," *IEEE Transactions on Vehicular Technology*, vol. 68, no. 8, pp. 8238–8242, 2019.
[101] L. Yang, J. X. Yang, W. W. Xie, *et al*., "Secrecy performance analysis of RIS-aided wireless communication systems," *IEEE Transactions on Vehicular Technology*, vol. 69, no. 10, pp. 12296–12300, 2020.
[102] H. L. Zhang, B. Y. Di, L. Y. Song, *et al*., "Reconfigurable intelligent surfaces assisted communications with limited phase shifts: How many phase shifts are enough?," *IEEE Transactions on Vehicular Technology*, vol. 69, no. 4, pp. 4498–4502, 2020.
[103] C. W. Huang, A. Zappone, G. C. Alexandropoulos, *et al*., "Reconfigurable intelligent surfaces for energy efficiency in wireless communication," *IEEE Transactions on Wireless Communications*, vol. 18, no. 8, pp. 4157–4170, 2019.
[104] Q. Q. Wu and R. Zhang, "Intelligent reflecting surface enhanced wireless network via joint active and passive beamforming," *IEEE Transactions on Wireless Communications*, vol. 18, no. 11, pp. 5394–5409, 2019.
[105] S. H. Zhang, H. L. Zhang, B. Y. Di, *et al*., "Intelligent Omni-surfaces: Ubiquitous wireless transmission by reflective-refractive metasurfaces," *IEEE Transactions on Wireless Communications*, vol. 21, no. 1, pp. 219–233, 2022.
[106] J. P. Qiao and M. S. Alouini, "Secure transmission for intelligent reflecting surface-assisted mmWave and terahertz systems," *IEEE Wireless Communications Letters*, vol. 9, no. 10, pp. 1743–1747, 2020.
[107] E. Basar, "Reconfigurable intelligent surfaces for Doppler effect and multipath fading mitigation," *Frontiers in Communications and Networks*, vol. 2, article no. 672857, 2021.
[108] F. Liu, O. Tsilipakos, A. Pitilakis, *et al*., "Intelligent metasurfaces with continuously tunable local surface impedance for multiple reconfigurable functions," *Physical Review Applied*, vol. 11, no. 4, article no. 044024, 2019.
[109] P. del Hougne, M. Fink, and G. Lerosey, "Optimally diverse communication channels in disordered environments with tuned randomness," *Nature Electronics*, vol. 2, no. 1, pp. 36–41, 2019.
[110] G. C. Trichopoulos, P. Theofanopoulos, B. Kashyap, *et al*., "Design and evaluation of reconfigurable intelligent surfaces in real-world environment," *IEEE Open Journal of the Communications Society*, vol. 3, pp. 462–474, 2022.
[111] T. Sleasman, M. F. Imani, M. Boyarsky, *et al*., "Computational through-wall imaging using a dynamic metasurface antenna," *OSA Continuum*, vol. 2, no. 12, pp. 3499–3513, 2019.
[112] Y. L. Zheng, K. Chen, Z. Y. Xu, *et al*., "Metasurface-assisted wireless communication with physical level information encryption," *Advanced Science*, vol. 9, no. 34, article no. 2204558, 2022.
[113] W. K. Tang, J. Y. Dai, M. Z. Chen, *et al*., "MIMO transmission through reconfigurable intelligent surface: System design, analysis, and implementation," *IEEE Journal on Selected Areas in Communications*, vol. 38, no. 11, pp. 2683–2699, 2020.
[114] J. Y. Dai, W. K. Tang, L. X. Yang, *et al*., "Realization of multi-modulation schemes for wireless communication by time-domain digital coding metasurface," *IEEE Transactions on Antennas and Propagation*, vol. 68, no. 3, pp. 1618–1627, 2020.
[115] J. Zhao, X. Yang, J. Y. Dai, *et al*., "Programmable time-domain digital-coding metasurface for non-linear harmonic manipulation and new wireless communication systems," *National Science Review*, vol. 6, no. 2, pp. 231–238, 2019.
[116] M. Z. Chen, W. K. Tang, J. Y. Dai, *et al*., "Accurate and broadband manipulations of harmonic amplitudes and phases to reach 256 QAM millimeter-wave wireless communications by time-domain digital coding metasurface," *National Science Review*, vol. 9, no. 1, article no. nwab134, 2022.
[117] E. Björnson, Ö. Özdogan, and E. G. Larsson, "Reconfigurable intelligent surfaces: Three myths and two critical questions," *IEEE Communications Magazine*, vol. 58, no. 12, pp. 90–96, 2020.
[118] Y. W. Liu, X. Liu, X. D. Mu, *et al*., "Reconfigurable intelligent surfaces: Principles and opportunities," *IEEE Communications Surveys & Tutorials*, vol. 23, no. 3, pp. 1546–1577, 2021.
[119] S. Basharat, M. Khan, M. Iqbal, *et al*., "Exploring reconfigurable

intelligent surfaces for 6G: State-of-the-art and the road ahead," *IET Communications*, vol. 16, no. 13, pp. 1458–1474, 2022.
[120] Q. Cheng, L. Zhang, J. Y. Dai, *et al*., "Reconfigurable intelligent surfaces: Simplified-architecture transmitters—From theory to implementations," *Proceedings of the IEEE*, vol. 110, no. 9, pp. 1266–1289, 2022.
[121] L. L. Li, H. T. Zhao, C. Liu, *et al*., "Intelligent metasurfaces: Control, communication and computing," *eLight*, vol. 2, no. 1, article no. 7, 2022.
[122] Q. He, S. L. Sun, and L. Zhou, "Tunable/reconfigurable metasurfaces: Physics and applications," *Research*, vol. 2019, article no. 1849272, 2019.
[123] Y. Saifullah, Y. J. He, A. Boag, *et al*., "Recent progress in reconfigurable and intelligent metasurfaces: A comprehensive review of tuning mechanisms, hardware designs, and applications," *Advanced Science*, vol. 9, no. 33, article no. 2203747, 2022.
[124] H. T. Chen, W. J. Padilla, M. J. Cich, *et al*., "A metamaterial solid-state terahertz phase modulator," *Nature Photonics*, vol. 3, no. 3, pp. 148–151, 2009.
[125] J. Zhang, H. Zhang, W. X. Yang, *et al*., "Dynamic scattering steering with grapheme-based coding metamirror," *Advanced Optical Materials*, vol. 8, no. 19, article no. 2000683, 2020.
[126] G. K. Shirmanesh, R. Sokhoyan, P. C. Wu, *et al*., "Electro-optically tunable multifunctional metasurfaces," *ACS Nano*, vol. 14, no. 6, pp. 6912–6920, 2020.
[127] Q. Wang, X. G. Zhang, H. W. Tian, *et al*., "Millimeter-wave digital coding metasurfaces based on nematic liquid crystals," *Advanced Theory and Simulations*, vol. 2, no. 12, article no. 1900141, 2019.
[128] N. Zhang, K. Chen, Y. L. Zheng, *et al*., "Programmable coding metasurface for dual-band independent real-time beam control," *IEEE Journal on Emerging and Selected Topics in Circuits and Systems*, vol. 10, no. 1, pp. 20–28, 2020.
[129] H. L. Wang, H. F. Ma, M. Chen, *et al*., "A reconfigurable multifunctional metasurface for full-space control of electromagnetic waves," *Advanced Functional Materials*, vol. 31, no. 25, article no. 2100275, 2021.
[130] K. Chen, Y. J. Feng, F. Monticone, *et al*., "A reconfigurable active Huygens' metalens," *Advanced Materials*, vol. 29, no. 17, article no. 1606422, 2017.
[131] J. C. Liang, Q. Cheng, Y. Gao, *et al*., "An angle-insensitive 3-bit reconfigurable intelligent surface," *IEEE Transactions on Antennas and Propagation*, vol. 70, no. 10, pp. 8798–8808, 2022.
[132] H. K. Kim, D. Lee, and S. Lim, "Frequency-tunable metamaterial absorber using a varactor-loaded fishnet-like resonator," *Applied Optics*, vol. 55, no. 15, pp. 4113–4118, 2016.
[133] Y. Kim, P. C. Wu, R. Sokhoyan, *et al*., "Phase modulation with electrically tunable vanadium dioxide phase-change metasurfaces," *Nano Letters*, vol. 19, no. 6, pp. 3961–3968, 2019.
[134] J. Shabanpour, "Programmable anisotropic digital metasurface for independent manipulation of dual-polarized THz waves based on a voltage-controlled phase transition of VO_2 microwires ," *Journal of Materials Chemistry C*, vol. 8, no. 21, pp. 7189–7199, 2020.
[135] Y. F. Wang, P. Landreman, D. Schoen, *et al*., "Electrical tuning of phase-change antennas and metasurfaces," *Nature Nanotechnology*, vol. 16, no. 6, pp. 667–672, 2021.
[136] S. Abdollahramezani, O. Hemmatyar, M. Taghinejad, *et al*., "Electrically driven reprogrammable phase-change metasurface reaching 80% efficiency," *Nature Communications*, vol. 13, no. 1, article no. 1696, 2022.
[137] Y. Z. Hu, T. Jiang, J. H. Zhou, *et al*., "Ultrafast terahertz frequency and phase tuning by all-optical molecularization of metasurfaces," *Advanced Optical Materials*, vol. 7, no. 22, article no. 1901050, 2019.
[138] P. P. Vabishchevich, A. Vaskin, N. Karl, *et al*., "Ultrafast all-optical diffraction switching using semiconductor metasurfaces," *Applied Physics Letters*, vol. 118, no. 21, article no. 211105, 2021.
[139] A. C. Tasolamprou, A. D. Koulouklidis, C. Daskalaki, *et al*., "Experimental demonstration of ultrafast THz modulation in a graphene-based thin film absorber through negative photoinduced conductivity," *ACS Photonics*, vol. 6, no. 3, pp. 720–727, 2019.
[140] P. J. Guo, R. D. Schaller, J. B. Ketterson, *et al*., "Ultrafast switching of tunable infrared plasmons in indium tin oxide nanorod arrays with large absolute amplitude," *Nature Photonics*, vol. 10, no. 4, pp. 267–273, 2016.
[141] M. Taghinejad, H. Taghinejad, Z. H. Xu, *et al*., "Ultrafast control of phase and polarization of light expedited by hot-electron transfer," *Nano Letters*, vol. 18, no. 9, pp. 5544–5551, 2018.
[142] M. K. Liu, H. Y. Hwang, H. Tao, *et al*., "Terahertz-field-induced insulator-to-metal transition in vanadium dioxide metamaterial," *Nature*, vol. 487, no. 7407, pp. 345–348, 2012.
[143] A. Leitis, A. Heßler, S. Wahl, *et al*., "All-dielectric programmable Huygens' metasurfaces," *Advanced Functional Materials*, vol. 30, no. 19, article no. 1910259, 2020.
[144] P. Pitchapp., A. Kumar, S. Prakash, *et al*., "Chalcogenide phase change material for active terahertz photonics," *Advanced Materials*, vol. 31, no. 12, article no. 1808157, 2019.
[145] X. G. Zhang, Y. L. Sun, B. C. Zhu, *et al*., "A metasurface-based light-to-microwave transmitter for hybrid wireless communications," *Light:Science & Applications*, vol. 11, no. 1, article no. 126, 2022.
[146] X. H. Yin, T. Steinle, L. L. Huang, *et al*., "Beam switching and bifocal zoom lensing using active plasmonic metasurfaces," *Science & Applications*, vol. 6, no. 7, article no. e17016, 2017.
[147] K. Sun, C. A. Riedel, A. Urbani, *et al*., "VO_2 thermochromic metamaterial-based smart optical solar reflector ," *ACS Photonics*, vol. 5, no. 6, pp. 2280–2286, 2018.
[148] T. Driscoll, S. Palit, M. M. Qazilbash, *et al*., "Dynamic tuning of an infrared hybrid-metamaterial resonance using vanadium dioxide," *Applied Physics Letters*, vol. 93, no. 2, article no. 024101, 2008.
[149] H. T. Chen, H. Yang, R. Singh, *et al*., "Tuning the resonance in high-temperature superconducting terahertz metamaterials," *Physical Review Letters*, vol. 105, no. 24, article no. 247402, 2010.
[150] M. Rahmani, L. Xu, A. E. Miroshnichenko, *et al*., "Reversible thermal tuning of all-dielectric metasurfaces," *Advanced Functional Materials*, vol. 27, no. 31, article no. 1700580, 2017.
[151] H. B. Wu, Q. L. Luo, H. J. Chen, *et al*., "Magnetically controllable nonreciprocal Goos-Hänchen shiftsupported by a magnetic plasmonic gradient metasurface," *Physical Review A*, vol. 99, no. 3, article no. 033820, 2019.
[152] M. Lei, Y. N. Feng, Q. M. Wang, *et al*., "Magnetically tunable metamaterial perfect absorber," *Journal of Applied Physics*, vol. 119, no. 24, article no. 244504, 2016.
[153] A. E. Serebryannikov, A. Lakhtakia, and E. Ozbay, "Characteristic attributes of multiple cascaded terahertz metasurfaces with magnetically tunable subwavelength resonators," *Annalen der Physik*, vol. 530, no. 3, article no. 1700252, 2018.
[154] S. S. Liu, Y. Long, C. Y. Liu, *et al*., "Bioinspired adaptive microplate arrays for magnetically tuned optics," *Advanced Optical Materials*, vol. 5, no. 11, article no. 1601043, 2017.
[155] J. Y. Ou, E. Plum, J. F. Zhang, *et al*., "An electromechanically reconfigurable plasmonic metamaterial operating in the near-infrared," *Nature Nanotechnology*, vol. 8, no. 4, pp. 252–255, 2013.
[156] H. S. Ee and R. Agarwal, "Tunable metasurface and flat optical zoom lens on a stretchable substrate," *Nano Letters*, vol. 16, no. 4, pp. 2818–2823, 2016.
[157] L. B. Yan, W. M. Zhu, M. F. Karim, *et al*., "0.2 λ_0 thick adaptive retroreflector made of spin-locked metasurface," *Advanced Materials*, vol. 30, no. 39, article no. 1802721, 2018.
[158] S. Sun, W. H. Yang, C. Zhang, *et al*., "Real-time tunable colors from microfluidic reconfigurable all-dielectric metasurfaces," *ACS Nano*, vol. 12, no. 3, pp. 2151–2159, 2018.
[159] C. Li, J. B. Wu, S. L. Jiang, *et al*., "Electrical dynamic modulation of THz radiation based on superconducting metamaterials," *Applied Physics Letters*, vol. 111, no. 9, article no. 092601, 2017.

[160] K. Shih, P. Pitchapp., M. Manjapp., *et al*., "Active MEMS metamaterials for THz bandwidth control," *Applied Physics Letters*, vol. 110, no. 16, article no. 161108, 2017.
[161] M. Li, L. Shen, L. Q. Jing, *et al*., "Origami metawall: Mechanically controlled absorption and deflection of light," *Advanced Science*, vol. 6, no. 23, article no. 1901434, 2019.
[162] S. Bildik, S. Dieter, C. Fritzsch, *et al*., "Reconfigurable folded reflectarray antenna based upon liquid crystal technology," *IEEE Transactions on Antennas and Propagation*, vol. 63, no. 1, pp. 122–132, 2015.
[163] M. H. Dahri, M. H. Jamaluddin, M. I. Abbasi, *et al*., "A review of wideband reflectarray antennas for 5G communication systems," *IEEE Access*, vol. 5, pp. 17803–17815, 2017.
[164] J. Ning, K. Chen, W. B. Zhao, *et al*., "An ultrathin tunable metamaterial absorber for lower microwave band based on magnetic nanomaterial," *Nanomaterials*, vol. 12, no. 13, article no. 2135, 2022.
[165] X. Yang, S. H. Xu, F. Yang, *et al*., "A broadband high-efficiency reconfigurable reflectarray antenna using mechanically rotational elements," *IEEE Transactions on Antennas and Propagation*, vol. 65, no. 8, pp. 3959–3966, 2017.
[166] E. Vassos, J. Churm, and A. Feresidis, "Ultra-low-loss tunable piezoelectric-actuated metasurfaces achieving 360° or 180° dynamic phase shift at millimeter-waves," *Scientific Reports*, vol. 10, no. 1, article no. 15679, 2020.
[167] X. Yang, S. H. Xu, F. Yang, *et al*., "A mechanically reconfigurable reflectarray with slotted patches of tunable height," *IEEE Antennas and Wireless Propagation Letters*, vol. 17, no. 4, pp. 555–558, 2018.
[168] W. Lee and Y. J. Yoon, "A broadband dual-metallic-reflectarray antenna for millimeter-wave applications," *IEEE Antennas and Wireless Propagation Letters*, vol. 16, pp. 856–859, 2017.
[169] V. F. Fusco, "Mechanical beam scanning reflectarray," *IEEE Transactions on Antennas and Propagation*, vol. 53, no. 11, pp. 3842–3844, 2005.
[170] R. Y. Deng, F. Yang, S. H. Xu, *et al*., "A 100-GHz metal-only reflectarray for high-gain antenna applications," *IEEE Antennas and Wireless Propagation Letters*, vol. 15, pp. 178–181, 2016.
[171] Q. Hu, J. M. Zhao, K. Chen, *et al*., "An intelligent programmable Omni-metasurface," *Laser & Photonics Reviews*, vol. 16, no. 6, article no. 2100718, 2022.
[172] W. K. Tang, M. Z. Chen, J. Y. Dai, *et al*., "Wireless communications with programmable metasurface: New paradigms, opportunities, and challenges on transceiver design," *IEEE Wireless Communications*, vol. 27, no. 2, pp. 180–187, 2020.
[173] S. Foo, "Liquid-crystal reconfigurable metasurface reflectors," in *Proceedings of the 2017 IEEE International Symposium on Antennas and Propagation & USNC/URSI National Radio Science Meeting*, San Diego, CA, USA, pp. 2069–2070, 2017.
[174] C. Liaskos, A. Tsioliaridou, and S. Ioannidis, "Towards a circular economy via intelligent metamaterials," in *Proceedings of the 2018 IEEE 23rd International Workshop on Computer Aided Modeling and Design of Communication Links and Networks*, Barcelona, Spain, pp. 1–6, 2018.
[175] L. L. Dai, B. C. Wang, M. Wang, *et al*., "Reconfigurable intelligent surface-based wireless communications: Antenna design, prototyping, and experimental results," *IEEE Access*, vol. 8, pp. 45913–45923, 2020.
[176] J. Y. Lau and S. V. Hum, "A wideband reconfigurable transmitarray element," *IEEE Transactions on Antennas and Propagation*, vol. 60, no. 3, pp. 1303–1311, 2012.
[177] X. Tan, Z. Sun, D. Koutsonikolas, *et al.* , "Enabling indoor mobile millimeter-wave networks based on smart reflect-arrays," in *Proceedings of the 2018 IEEE Conference on Computer Communications*, Honolulu, HI, USA, pp. 270–278, 2018.
[178] H. T. Zhao, Y. Shuang, M. L. Wei, *et al*., "Metasurface-assisted massive backscatter wireless communication with commodity Wi-Fi signals," *Nature Communications*, vol. 11, no. 1, article no. 3926, 2020.
[179] V. Arun and H. Balakrishnan, "RFocus: Beamforming using thousands of passive antennas," in *Proceedings of the 17th USENIX Symposium on Networked Systems Design and Implementation*, Santa Clara, CA, USA, pp. 1047–1062, 2020.
[180] K. Tang, N. Zhang, K. Chen, *et al*., "Reconfigurable intelligent surface enhancing in-door wireless communication," in *Proceedings of the 2021 IEEE International Workshop on Electromagnetics: Applications and Student Innovation Competition*, Guangzhou, China, pp. 1–3, 2021.
[181] L. Zhang, M. Z. Chen, W. K. Tang, *et al*., "A wireless communication scheme based on space- and frequency-division multiplexing using digital metasurfaces," *Nature Electronics*, vol. 4, no. 3, pp. 218–227, 2021.
[182] D. Kitayama, Y. Hama, K. Goto, *et al*., "Transparent dynamic metasurface for a visually unaffected reconfigurable intelligent surface: Controlling transmission/reflection and making a window into an RF lens," *Optics Express*, vol. 29, no. 18, pp. 29292–29307, 2021.
[183] J. W. Tang, M. Y. Cui, S. H. Xu, *et al*., "Transmissive RIS for 6G communications: Design, prototyping, and experimental demonstrations," *arXiv preprint*, arXiv: 2206.15133, 2022.
[184] A. Araghi, M. Khalily, M. Safaei, *et al*., "Reconfigurable intelligent surface (RIS) in the Sub-6 GHz band: Design, implementation, and real-world demonstration," *IEEE Access*, vol. 10, pp. 2646–2655, 2022.
[185] H. Jeong, E. Park, R. Phon, *et al*., "Mechatronic reconfigurable intelligent-surface-driven indoor fifth-generation wireless communication," *Advanced Intelligent Systems*, vol. 4, no. 12, article no. 2200185, 2022.
[186] F. Liu, A. Pitilakis, M. S. Mirmoosa, *et al.* , "Programmable metasurfaces: State of the art and prospects," in *Proceedings of the 2018 IEEE International Symposium on Circuits and Systems*, Florence, Italy, pp. 1–5, 2018.
[187] M. D. Renzo, M. Debbah, D. T. Phan-Huy, *et al*., "Smart radio environments empowered by reconfigurable AI meta-surfaces: An idea whose time has come," *EURASIP Journal on Wireless Communications and Networking*, vol. 2019, no. 1, article no. 129, 2019.
[188] C. W. Huang, S. Hu, G. C. Alexandropoulos, *et al*., "Holographic MIMO surfaces for 6G wireless networks: Opportunities, challenges, and trends," *IEEE Wireless Communications*, vol. 27, no. 5, pp. 118–125, 2020.
[189] Y. C. Liang, R. Z. Long, Q. Q. Zhang, *et al*., "Large intelligent surface/antennas (LISA): Making reflective radios smart," *Journal of Communications and Information Networks*, vol. 4, no. 2, pp. 40–50, 2019.
[190] D. Bhandari, C. A. Murthy, and S. K. Pal, "Genetic algorithm with elitist model and its convergence," *International Journal of Pattern Recognition and Artificial Intelligence*, vol. 10, no. 6, pp. 731–747, 1996.
[191] X. D. Meng, R. X. Liu, H. C. Chu, *et al*., "Through-wall wireless communication enabled by a metalens," *Physical Review Applied*, vol. 17, no. 6, article no. 064027, 2022.
[192] B. Sanz-Izquierdo and E. A. Parker, "Dual polarized reconfigurable frequency selective surfaces," *IEEE Transactions on Antennas and Propagation*, vol. 62, no. 2, pp. 764–771, 2014.
[193] M. Bouslama, M. Traii, T. A. Denidni, *et al*., "Beam-switching antenna with a new reconfigurable frequency selective surface," *IEEE Antennas and Wireless Propagation Letters*, vol. 15, pp. 1159–1162, 2016.
[194] Z. J. Zhang, L. L. Dai, X. B. Chen, *et al*., "Active RIS vs. passive RIS: Which will prevail in 6G?," *IEEE Transactions on Communications*, vol. 71, no. 3, pp. 1707–1725, 2023.
[195] Q. Ma, L. Chen, H. B. Jing, *et al*., "Controllable and programmable nonreciprocity based on detachable digital coding metasurface," *Advanced Optical Materials*, vol. 7, no. 24, article no. 1901285, 2019.
[196] S. Taravati and G. V. Eleftheriades, "Full-duplex reflective beamsteering metasurface featuring magnetless nonreciprocal amplifica-

tion," *Nature Communications*, vol. 12, no. 1, article no. 4414, 2021.

[197] S. Taravati and G. V. Eleftheriades, "Programmable nonreciprocal meta-prism," *Scientific Reports*, vol. 11, no. 1, article no. 7377, 2021.

[198] R. Q. Liu, Q. Q. Wu, M. D. Renzo, *et al*., "A path to smart radio environments: An industrial viewpoint on reconfigurable intelligent surfaces," *IEEE Wireless Communications*, vol. 29, no. 1, pp. 202–208, 2022.

[199] S. M. Gong, X. Lu, D. T. Hoang, *et al*., "Toward smart wireless communications via intelligent reflecting surfaces: A contemporary survey," *IEEE Communications Surveys & Tutorials*, vol. 22, no. 4, pp. 2283–2314, 2020.

[200] C. Liaskos, L. Mamatas, A. Pourdamghani, *et al*., "Software-defined reconfigurable intelligent surfaces: From theory to end-to-end implementation," *Proceedings of the IEEE*, vol. 110, no. 9, pp. 1466–1493, 2022.

Yijun Feng received the Ph.D. degree from the Department of Electronic Science and Engineering, Nanjing University, China, in 1992. Since then, he has been a faculty member and is a Full Professor and Deputy Dean of the School of Electronic Science and Engineering, Nanjing University. From September 1995 to July 1996, he was a Visiting Scientist at the Physics Department of Technical University of Denmark, Denmark. From August 2001 to August 2002, he was a Visiting Researcher at the University of California, Berkeley, USA. His research interests include EM metamaterials and their application to microwave and photonic devices, EM wave theory, and novel microwave functional materials.

Dr. Feng has served as the General Co-Chair of 2018 IEEE International Workshop on Antenna Technology, and Technical Program Co-Chair of 2013 International Symposium on Antennas and Propagation. He is the recipient of the 2010 Science and Technology Award (first grade) of Jiangsu Province, and the 2021 Science and Technology Award (first grade) of Shanxi Province, China. He has authored or co-authored over 200 peer-reviewed journal papers and over 160 refereed international conference papers. (Email: yjfeng@nju.edu.cn)

Qi Hu received the B.S. degree in communication engineering from the Communication University of China, Beijing, China, in 2019. She is currently pursuing the Ph.D. degree in electronic science and technology with Nanjing University, Nanjing, China. Her current research focuses on metasurfaces. (Email: hq1111@smail.nju.edu.cn)

Kai Qu received the B.S. degree in optical engineering from the Harbin Institute of Technology, Harbin, China, in 2019. He is currently pursuing the Ph.D. degree in electronic science and technology with Nanjing University, Nanjing, China. His current research focuses on the multifunctional metasurfaces. (Email: kqu@smail.nju.edu.cn)

Weixu Yang received the B.S. degree in communication engineering from Nanjing University of Science and Technology, Nanjing, China, in 2019. He is currently pursuing the Ph.D. degree in electronic science and technology with Nanjing University. His current research interests include electromagnetic metasurfaces, reflectarray/transmitarray antennas, and millimeter-wave antennas. (Email: wxyang@smail.nju.edu.cn)

Yilin Zheng received the B.S. degree in telecommunications engineering from Nanjing University, Nanjing, China, in 2018, where she is currently pursuing the Ph.D. degree in electronic science and technology under the supervision of Prof. Yijun Feng. She has published 4 peer-reviewed first-author journal articles. Her current research interests include origami-inspired metamaterials for beam manipulation and wireless communication based on metamaterials. (Email: DG20230062@smail.nju.edu.cn)

Ke Chen received the B.S. and Ph.D. degrees in electronic science and engineering from Nanjing University, Nanjing, China, in 2012 and 2017, respectively. He is currently an Associate Professor at the Department of Electronic Engineering, School of Electronic Science and Engineering, Nanjing University. His research interests include electromagnetic metamaterials and metasurfaces and their applications to wireless communication and photonic devices. Dr. Chen is the recipient of the Best Excellent Doctoral Dissertation Award of China Education Society of Electronics in 2018, the Young Scientist Award of URSI General Assembly and Scientific Symposium (GASS) in 2021, and the Young Scientist Award of International Applied Computational Electromagnetics Society (ACES) in 2021. He has authored or co-authored over 70 peer-reviewed journal articles and over 60 refereed international conference papers. (Email: ke.chen@nju.edu.cn)